



Deposited via The University of Leeds.

White Rose Research Online URL for this paper:

<https://eprints.whiterose.ac.uk/id/eprint/241043/>

Version: Accepted Version

---

**Article:**

Iryo, T., Watling, D. and Hazelton, M. (Accepted: 2026) Impacts of within-day decision-making within a stochastic process traffic assignment model. Transportation Research Part B: Methodological. ISSN: 0191-2615 (In Press)

---

This is an author produced version of an article accepted for publication in Transportation Research Part B: Methodological, made available via the University of Leeds Research Outputs Policy under the terms of the Creative Commons Attribution License (CC-BY), which permits unrestricted use, distribution and reproduction in any medium, provided the original work is properly cited.

**Reuse**

This article is distributed under the terms of the Creative Commons Attribution (CC BY) licence. This licence allows you to distribute, remix, tweak, and build upon the work, even commercially, as long as you credit the authors for the original work. More information and the full terms of the licence here:

<https://creativecommons.org/licenses/>

**Takedown**

If you consider content in White Rose Research Online to be in breach of UK law, please notify us by emailing [eprints@whiterose.ac.uk](mailto:eprints@whiterose.ac.uk) including the URL of the record and the reason for the withdrawal request.

# Impacts of within-day decision-making within a stochastic process traffic assignment model

Takamasa Iryo<sup>a,\*</sup>, David Watling<sup>b</sup>, and Martin Hazelton<sup>c</sup>

<sup>a</sup>University of Tokyo, 7-3-1, Hongo, Bunkyo-ku, Tokyo, 113-8656, Japan

<sup>b</sup>University of Leeds, 34-40 University Road, Leeds, LS2 9JT, United Kingdom

<sup>c</sup>University of Otago, 730 Cumberland St., Dunedin, 9016, New Zealand

---

**Keywords:**

Markov process

day-to-day dynamics

within-day dynamics

stability analysis

Markov chain mixing time

Existing day-to-day models assume that travellers make decisions based on traffic conditions from previous days rather than those on the actual travel day. However, this approach cannot capture frequent within-day updates of travel information, significantly influencing both day-to-day and within-day dynamics. To address this, we proposed the concept of a within-day decision-making framework and developed a mathematically simple and concise Markovian-based model. Additionally, to characterise and quantify the impacts of the proposed model, we introduced three multi-faceted measures: the convergence speed towards the stationary distribution, its key characteristics, and the within-day adaptation capability, all designed to reflect the stability and resilience of the transport system. We conducted numerical experiments on the departure time choice problem in both a single-link network and the Sioux Falls network. The results clearly demonstrate the impacts of the proposed decision-making framework through the proposed measures, particularly highlighting its effects on the stability and resilience of the transport system.

---

## 1 Introduction

Day-to-day dynamical models describe how travellers adjust their behaviour over days in response to traffic situations in previous days, assuming models of travellers' adaptive behaviour. These models have a long history in transportation science, see, for example, Horowitz (1984), Chang and Mahmassani (1988), Friesz et al. (1996), Jin (2007), Yang and Zhang (2009), He et al. (2010), Friesz et al. (2011), Smith and Watling (2016), Li et al. (2019), Li et al. (2024), Cantarella et al. (2025). A particular class of such approaches are those that represent the system evolution as a stochastic process, in which travellers' adjustment behaviour, as well as potentially the physical network, are represented using *probabilistic* models.

---

\* Corresponding author. E-mail address: iryo@bin.t.u-tokyo.ac.jp.

These models have been investigated for many decades as a tool for analysing how transport systems change over days to determine their dynamical properties, such as whether and how these systems converge to a unique equilibrium distribution. Within this class, Markovian models assume that the traffic state in one day depends on a finite number of previous days' traffic states. Many studies have proposed and utilised Markovian day-to-day dynamical models, including e.g. Cascetta (1989), Cantarella and Cascetta (1995), Watling (1996), Hazelton (2002), Hazelton and Watling (2004), Watling and Cantarella (2013), Cantarella and Watling (2015), Parry et al. (2016), Watling and Hazelton (2018), Satsukawa et al. (2019), and Iryo et al. (2024).

The basic framework of Markovian day-to-day dynamical models is that travellers decide their behaviour depending on the traffic conditions that actually occurred on days in the *past*, i.e. *not* on the day they are travelling. This implies that they assume that travellers estimate the travel costs of different options, such as routes and departure times, by considering the traffic conditions on the past day(s). In addition, these models implicitly assume that travellers can choose any departure times on the day of travel. This framework is equivalent to assuming that the timing of the travellers' decision-making is not dynamically determined within a day, but is *statically* fixed at the beginning of the day of travel. We call such a framework the *static framework of travellers' decision-making*.

The static framework of travellers' decision-making is, however, not very useful in many situations, for example, as follows:

1. A situation in which travellers do not tend to reconsider their departure time at the start of the day, and instead normally defer any decision on changing departure time until later in the day. For example, a traveller departing regularly at 8.30 may first consider revising their decision at say 8.00, but then clearly this rules out earlier options than 8.00, even if they may have a higher utility.
2. A situation in which travellers' decisions can be affected by the latest information on the transport system. This point is essential in many applications, for example, when we evaluate:
  - (a) the benefits of new technologies that collect and process the most recent, accurate information for aiding travellers' best decisions;
  - (b) the restoration process of the transport system after an unpredictable incident, such as a traffic accident or a natural disaster.

In cases 2(a) and 2(b), travellers may intentionally defer their decision-making times to collect more accurate information and find a better alternative.

In all of the above situations (1, 2(a), 2(b)), the static assumption that travellers' decisions are fully determined before the day of travel begins is not applicable. Instead, we must adopt a setting in which travellers' *decisions* can occur at any point during the day of travel. The timing of these decisions then influences the available departure time options and the information they possess.

The idea that travellers' considered departure time options on one day may be restricted by previous daily experience is not a new one. Most notably, several authors have considered various forms of boundedly rational decision rules in a day-to-day dynamic, departure time choice setting (for example: Chen et al. (2021); Mahmassani and Chang (1986)). However, the rules adopted in these prior works are quite different from our focus, since these earlier works all fall within the static decision-making framework described above. That is to say, the consideration set of departure times on one day is determined by the historical experience of previous days.

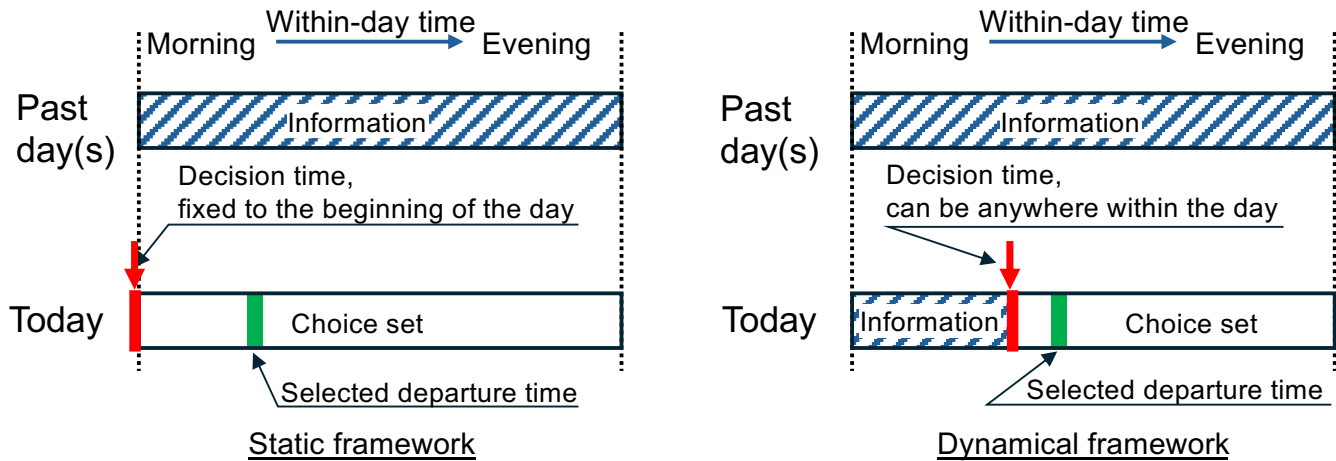


Figure 1: Schematic view of the static and dynamical frameworks of decision-making

To stipulate the situation in which travellers make decisions at any time in the day of travel, we instead propose a new framework for modelling travellers' behaviour, consisting of the following principles:

**Principle A – Decision time:** Travellers' choice behaviour is characterised by the within-day time when the choice is determined, referred to as the *decision time*.

**Principle B – Departure time:** Any alternative is associated with the time at which a traveller takes the action of this alternative. It is called the *departure time*.

**Principle C – Monotonic shrinking property of choice sets:** A traveller's choice set depends on the decision time. The choice set contains all alternatives whose departure time is not earlier than the decision time. This property implies that the size of each traveller's choice set decreases weakly monotonically over time.

**Principle D – Causality of information acquisition:** A traveller's choice depends solely on information that is potentially available at the decision time.

We call the framework consisting of these principles the *dynamical framework of travellers' decision-making*. When we want to derive a specific travel behaviour model based on this framework, it is necessary and sufficient to formulate the models describing how travellers determine their decision times for Principle A, determining departure times and formulating choice sets for Principles B and C, and modelling how information is processed depending on the traffic situation and how a traveller makes a choice depending on the information and choice set for Principle D. For example, if the decision time of all users is set to the beginning of the day of the trip and the information possessed by the traveller is assumed to depend on the traffic conditions one (or more) day(s) before the trip, the derived model is identical to a conventional day-to-day dynamical model based on the static framework. Figure 1 is a schematic view of the dynamical framework of travellers' decision-making, accompanied by the static one for comparison.

Although we would be able to consider a wide range of study topics related to the dynamical framework of decision-making proposed above, our main interest in the present paper is in *how the introduction of this framework impacts the dynamics of stochastic process traffic assignment models*. In particular, we are interested in understanding the three properties described as follows:

- (a) Convergence speed of the day-to-day dynamics towards the stationary distribution
- (b) Properties of the stationary distribution
- (c) The capability of within-day adaptation, reflecting the resilience of the transport system and its travellers after deviations from the normal state during the day

Property (b) is further categorised as follows:

1. The size of the stationary distribution: the stationary distribution corresponds to the equilibrium solution in the traffic assignment problem under a deterministic approach, so understanding its characteristics is as crucial as understanding the properties of equilibrium solutions, such as their uniqueness and stability. The uniqueness of the stationary distribution is guaranteed under weak conditions. However, it should be emphasised that a stationary distribution does not correspond to one specific state, but to a distribution across multiple states. In other words, the uniqueness of the stationary distribution does not carry the same implication as the uniqueness of the equilibrium solution, which would mean being able to predict a single, clearly specified future state. The purpose of introducing the size index is to understand the extent of variability in future states.
2. The instability index: when the stationary distribution of a Markov chain spreads over multiple states, the system's state continuously transitions dynamically within this distribution. This movement can be characterised by two types of behaviour: random fluctuations and stochastic periodicity caused by short-term correlations. See Figure 2 for a schematic comparison illustrating examples of these two behaviours. When stochastic periodicity dominates the movements, the system exhibits dynamic behaviour that goes beyond noise-induced variability. Such behaviour leads to short-range stochastic trends, which can generate seemingly periodic patterns, making it difficult for the system to remain stable in any particular state. The instability index is introduced to quantify the degree of such periodicity.
3. Travellers' behaviour changes within a day: the dynamical framework implies that travellers can change their decisions within a day. As noted in 2., the state of the system can continuously transition even within the stationary distribution. Therefore, although it may seem counterintuitive, such within-day changes in user behaviour can still remain within the stationary distribution. Therefore, it is crucial to check how it changes in the stationary distribution to understand how the dynamical framework affects travellers' behavioural adjustment processes.

The first two are related to the properties of the stationary distribution of the Markov process describing the day-to-day dynamics, and the last one is related to the within-day properties of the dynamics.

Properties (a), (b), and (c) are related to the reliability/stability and resilience of the transport system. (b) indicates the degree to which the transport system is unstable and unreliable. (a) and (c) characterise the convergence behaviour to a steady state, i.e. (a) the day-to-day convergence speed and (c) the within-day convergence capability. They both represent the extent to which the effects of various perturbations on the system dissipate over a period of days or hours, and are important properties for assessing the resilience of the transport system.

The purpose of this study is to investigate the impacts of the dynamical framework of decision-making on the above three properties (a), (b), and (c), which together measure the reliability/stability and resilience of the transport system. The main contributions of this study are as follows:

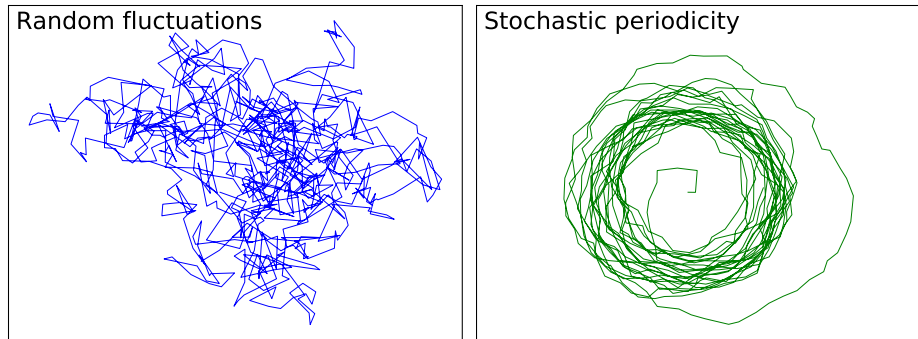


Figure 2: Schematic view of trajectories dominated by the random fluctuation (left) and stochastic periodicity (right) in the stationary distribution

- I. Proposing an essential but simple and generic form of the stochastic day-to-day dynamical model complying with the principles of the dynamical framework of decision-making, in the sense defined.
- II. Developing multi-faceted measures assessing properties (a), (b), and (c) for stochastic process models.
- III. Investigating the impacts of within-day decision-making within a framework of day-to-day dynamics modelled by I using the three measures introduced in II.

The structure of the present paper is as follows. Section 1 explained the motivation and aim of the present study. Section 2 explains the model specification. Section 3 introduces the measures for evaluating properties of stationary distributions. Section 4 presents numerical assessments using the single-link departure time choice problem. Section 5 discusses the challenges of extending the proposed framework to network-wide settings and presents approaches to achieve network-level scalability, with a case study of the Sioux Falls network. Section 6 concludes the paper and gives future directions.

## 2 Model specification

### 2.1 Basic framework of the model

We consider a transport system consisting of atomic travellers. The set of travellers is denoted by  $I$ , and the number of travellers is denoted by  $n$ . We do not consider a trip chain nor en-route updates of route choices in the present study; any traveller is assumed to select a single choice for a trip on the day. Each choice represents an alternative that a traveller uses for travelling, such as a route, a departure time, or a combination of a route and departure time, depending on the characteristics of the transport system and assumptions on travellers' behaviour. As is generally considered in the analysis of transport systems, this study also assumes that there is an interrelationship between user behaviour and the Level of Service (LOS) of the transport system, i.e. travellers' choices affect the transport system, thereby changing its LOS as represented by variables such as travel time, and in turn, this affects future travellers' choices. The set of all available choice options for traveller  $i \in I$  is denoted by  $C_i$ .

The introduction of the dynamical framework of decision-making implies that travellers' decisions and choices are characterised by both within-day time and date (day). As defined in Section 1, the within-day time when a decision is made is referred to as a *decision time*. To facilitate the description of this point,

we first introduce a tuple of time and date, namely  $(t, d)$ , where  $(t, d) \in S = T \times D$ ,  $T = \{1, 2, \dots, t^{\text{Max}}\}$ , and  $D$  is a set of positive integers. A natural lexicographical order relationship is defined on set  $S$ , namely, for  $(t_1, d_1), (t_2, d_2) \in S$ ,  $d_1 < d_2$  implies  $(t_1, d_1) < (t_2, d_2)$ , and  $t_1 < t_2$  and  $d_1 = d_2$  implies  $(t_1, d_1) < (t_2, d_2)$ . In addition, we define incremental and decremental operations on  $S$  as

$$(t, d) + \mathbf{1} = \begin{cases} (t + 1, d) & \text{if } t < t^{\text{Max}} \\ (1, d + 1) & \text{if } t = t^{\text{Max}} \end{cases} \quad (1)$$

$$(t, d) - \mathbf{1} = \begin{cases} (t - 1, d) & \text{if } t > 1 \\ (t^{\text{Max}}, d - 1) & \text{if } t = 1 \end{cases} \quad (2)$$

We also denote the initial epoch time, i.e. the first time slot of the first day by  $(1, 1)$ . When  $(t, d)$  is used as the sole argument of a function, the brackets will be omitted (e.g.  $f(t, d)$  instead of  $f((t, d))$ ) to simplify the notation.

Following Principles A – D explained in Section 1, we now formulate the details of the travellers' decisions and choices as follows:

1. **(Decision)** Travellers always have a choice in their minds about when and how to travel. We will refer to this as a *decision*. Traveller  $i$ 's decision at  $(t, d)$  (i.e. at the time  $t$  on day  $d$ ) is denoted by  $c_i(t, d) \in C_i$ . We assume that each decision consists of the decisions about the departure time and the route choices; the route choices may be omitted if only a single route is available, or replaced with other types of travel options such as transport modes or combinations of routes and modes. We introduce a tuple of the decisions of the departure time and the route to characterise the traveller's decision, namely:

$$c_i(t, d) = (\tau_i(t, d), r_i(t, d)), \quad (3)$$

where  $\tau_i(t, d) \in T$  and  $r_i(t, d) \in R_i$  are the traveller  $i$ 's decision of the departure time and route at  $(t, d)$ , respectively, and  $R_i$  is traveller  $i$ 's route choice set. We also introduce the vector forms of the decisions as follows:

$$\mathbf{c}(t, d) = (c_i(t, d))_{i \in I} = ((\tau_i(t, d), r_i(t, d)))_{i \in I} \quad (4)$$

$$\boldsymbol{\tau}(t, d) = (\tau_i(t, d))_{i \in I} \quad (5)$$

$$\mathbf{r}(t, d) = (r_i(t, d))_{i \in I}. \quad (6)$$

We also define  $C$  as the feasible set of  $\mathbf{c}(t, d)$ , which is the Cartesian product of  $C_i$  for all  $i \in I$ . Note that  $\mathbf{c}(t, d)$  indicates the decisions of travellers *after* their decision making at  $(t, d)$  is completed. Decisions at the epoch time, namely  $\mathbf{c}(1, 1)$ , will be given externally as an initial value of the dynamical model.  $\mathbf{c}(1, 1)$  is also called the *initial state*.

2. **(Initial decision making)** Travellers determine their decisions at the beginning of each day (i.e.  $t = 1$ ). It is called the *initial decision making*, and abbreviated *IDM*.
  - We consider two types of initial decision making, namely, (1) choose a decision from the choice set based on the condition of the transport system on the previous day, referred to as *updated initial decision making*, abbreviated as *uIDM*, and (2) adopt the choice on the previous day as the initial decision, referred to as *retained initial decision making*, abbreviated as *rIDM*.

Because rIDM corresponds to ‘no action’ in IDM, we do not use this term in the remainder of the paper. Unless otherwise stated, we use IDM to refer to uIDM throughout the paper. The set of travellers performing the updated initial decision making at the beginning of day  $d$  is denoted by  $I^I(d)$ .

- Travellers determine their initial decisions based on the LOS realised in the transport system on the previous day.
  - Travellers can select any departure time  $\tau_i$  in  $T$  during the IDM.
3. **(Within-day decision update)** Travellers may update their decisions at any time unless they have already departed. Such an update is called *within-day decision update*, abbreviated *WDU*. The set of travellers making a within-day decision at  $(t, d)$  is denoted by  $I^W(t, d)$ , where  $t > 1$ .
- Travellers may be able to update their decisions twice or more on the same day.
  - Travellers perform the WDU based on the latest information on the predicted LOS provided to the travellers.
  - Any choice selected through the WDU is restricted to those options whose departure time is not earlier than  $t$ . The choice set consisting of such choices is referred to as the *restricted choice set*, which is defined as

$$C_i(t) = \{(\tau, r) | \tau \geq t \text{ and } r \in R_i\}. \quad (7)$$

This invokes the shrinking property of the restricted choice set, i.e.  $t_1 \leq t_2 \Rightarrow C_i(t_1) \supseteq C_i(t_2)$ .

4. **(Finalising decisions and departing)** Traveller  $i$  makes the trip using the choice already decided once its departure time  $\tau_i(t, d)$  comes. Once travellers depart, they do not update their decisions until the day ends, i.e. the next chance of IDM.
- In every time slot, travellers first have a chance to perform the WDU before finalising their decisions and departing. For example, consider traveller  $i \in I^W(t, d)$  who have decided to depart at  $t$  until  $t - 1$  of day  $d$ , i.e.  $\tau_i(t - 1, d) = t$ . This traveller would depart at  $t$  if this decision is continuously kept to the next time slot, i.e.  $t$ . However, because this traveller has a chance to perform the WDU before departing,  $\tau_i(t, d)$  would be updated from  $\tau_i(t - 1, d)$ , which can be greater than  $t$  owing to Equation (7), resulting in deferred departure.
  - When  $t = t^{\text{Max}}$ , all travellers who have not departed must depart because  $\tau_i(t, d) \leq t^{\text{Max}}$  at all times. This implies that  $c_i(t^{\text{Max}}, d)$  indicates traveller  $i$ 's actual choice on day  $d$ .

Obviously, letting  $I^W(t, d) = \emptyset$  for all  $t > 1$  and  $d$ , the model falls back to that with the static framework of travellers' decision-making.

To describe both the initial and within-day decisions defined in items 2 and 3 at once, we introduce the set denoted by  $I(t, d)$ , which is defined as

$$I(t, d) = \begin{cases} I^I(t, d) & \text{if } t = 1 \\ I^W(t, d) & \text{otherwise.} \end{cases} \quad (8)$$

The definition of  $I(t, d)$  can be arbitrary; however, as travellers do not perform the WDU after they depart, the following must hold at all times:

$$\tau_i(t, d) < t \Rightarrow i \notin I(t, d). \quad (9)$$

## 2.2 Formulating the dynamical model based on the concept of OTIS

The basic framework of the model explained in the last section is insufficient to propose an explicit formula for the dynamical model because it does not contain how the information on the LOS is provided and how travellers react to this. To fill this gap and complete the formulation of the model, we now introduce the concept called *oracle traffic information system*, abbreviated *OTIS* (which is similar in principle, though not in detail, to the idealised system of Friesz et al. (1994)).

The OTIS is capable of:

- perfectly collecting travellers' latest decisions in real-time,
- perfectly obtaining performance parameters of the transport system, e.g. capacity of roads – not only those in the current situation but also those in the future on the same day,
- performing a perfectly accurate simulation of the transport system and obtaining perfect (i.e. oracle) predictions of the LOS, and providing them to travellers in real-time.

To formulate the OTIS, denote the predicted LOS at  $(t, d)$  by  $\mathbf{w}(t, d)$  and the performance parameters of the transport system by  $\xi$ . Then, the assumptions on OTIS stated above invoke the following formula:

$$\mathbf{w}(t, d) = \Phi(\mathbf{c}(t, d), \xi), \quad (10)$$

where  $\Phi$  is the function representing the simulator for OTIS that provides accurate outputs based on the given data, namely  $\mathbf{c}(t, d)$  and  $\xi$ . Note that  $\mathbf{w}(t, d)$  includes information on the LOS for the entire day  $d$ , which is predicted by OTIS at time  $t$ ;  $t$  does **not** indicate the time at which the LOS is observed.

As the simulator and input data are perfectly accurate, the simulator's output at the end of the day (i.e.  $t = t^{\text{Max}}$ ) is identical to the actual LOS in the real transport system. Therefore,  $\mathbf{w}(t, d)$  can be regarded as a prediction of the LOS in the WDU if  $t < t^{\text{Max}}$ , otherwise, it can be considered as the actual LOS on the previous day in IDM. This consideration naturally invokes the following mechanism:  $c_i((t, d) + \mathbf{1})$  depends on  $\mathbf{w}(t, d)$  in the IDM/WDU, resulting in the following formula relating  $c_i((t, d) + \mathbf{1})$  and  $\mathbf{w}(t, d)$ :

$$c_i((t, d) + \mathbf{1}) = \begin{cases} \chi_i(\mathbf{w}(t, d), C_i^+(t)) & \text{if } i \in I(t, d) \\ c_i(t, d) & \text{otherwise,} \end{cases} \quad (11)$$

where

$$C_i^+(t) = \begin{cases} C_i(t+1) & \text{if } t < t^{\text{Max}} \\ C_i(1) & \text{if } t = t^{\text{Max}} \end{cases} \quad (12)$$

is the restricted choice set at the next time step, or the beginning of the day if the current time step is  $t^{\text{Max}}$ .  $\chi_i(\mathbf{w}(t, d), C_i^+(t))$  returns a new decision of traveller  $i$  based on the LOS  $\mathbf{w}(t, d)$  and the restricted choice set.

We adopt standard random utility theory to formulate  $\chi_i(\mathbf{w}(t, d), C_i^+(t))$ . It is defined as

$$\chi_i(\mathbf{w}(t, d), C_i^+(t)) = \arg \max_{c \in C_i^+(t, d)} \{v_{ic}(\mathbf{w}(t, d)) + \varepsilon_{ci}(t, d)\}, \quad (13)$$

where  $\varepsilon_i(t, d) = (\varepsilon_{ci}(t, d))_{c \in C_i}$  is a random term vector and  $v_{ic}(\mathbf{w}(t, d))$  is traveller  $i$ 's systematic component of utility for choice  $c$  with  $\mathbf{w}(t, d)$  given.  $\varepsilon_{ci}(t, d)$  follows a certain distribution like the normal or

Gumbel distribution, and may be correlated across alternatives if the corresponding choices are similar. We assume that  $\varepsilon_{c_i}(t, d)$  is a real-valued random variable with unbounded support, which implies that  $\text{Prob}(\chi_i(\mathbf{w}(t, d), C_i^+(t)) = c) > 0$  for all  $c \in C_i$ . Note that the  $\varepsilon_{c_i}(t, d)$  drawn at different  $(t, d)$  are assumed independent of each other.

Combining Equations (10) – (13), we finally obtain the recurrence equation describing both within-day and day-to-day dynamics at once, i.e.

$$c_i((t, d) + \mathbf{1}) = \begin{cases} \chi_i(\Phi(\mathbf{c}(t, d), \boldsymbol{\xi}), C_i^+(t)) & \text{if } i \in I(t, d) \\ c_i(t, d) & \text{otherwise .} \end{cases} \quad (14)$$

Note that, as function  $\chi_i$  includes random variables, Equation (14) does not return a deterministic value but a stochastic one even if all other items are deterministic. Therefore, we consider  $c_i(t, d)$  as a random variable throughout the present paper.  $I(t, d)$  can also be stochastically defined if the IDM/WDU includes a random property, e.g. if travellers performing the IDU/WDU are randomly drawn.

### 2.3 Converting the dynamical model to a Markov-chain based model

The dynamics formulated by Equation (14) do not imply the existence of a Markov chain whose state variable is  $\mathbf{c}(t, d)$  because this variable depends not only on  $\mathbf{c}(t, d)$  but also on  $C_i^+(t)$  and  $I(t, d)$ . To employ the methodologies for Markov-chain models for evaluating the impacts of the within-day decision-making framework, we introduce an auxiliary model of  $I(t, d)$  so that  $I(t, d)$  will depend on  $\mathbf{c}(t, d)$  and  $t$  only. To facilitate this, we first define a set including travellers who have already departed before  $t$ , namely

$$I^{\text{dept}}(\mathbf{c}(t, d), t) = \{i \mid \tau_i(t, d) < t\}. \quad (15)$$

Using this, we assume that  $I(t, d)$  depends on  $\mathbf{w}(t, d)$ ,  $I^{\text{dept}}(\mathbf{c}(t, d), t)$ , and  $t$  only, which is denoted by

$$I(t, d) = \tilde{I}(\mathbf{w}(t, d), I^{\text{dept}}(\mathbf{c}(t, d), t), t). \quad (16)$$

This model implies that whether a traveller performs the IDM/WDU at  $t$  or not depends on the current prediction of the LOS and  $t$  itself, but does not depend on how many times this traveller has performed the IDM/WDU before. In this sense, this model has a memoryless property of Markov chains. Because we need to exclude departed travellers from  $I(t, d)$ ,  $I^{\text{dept}}(\mathbf{c}(t, d), t)$  must be set as an input of this model. Substituting Equation (10) into Equation (16), we have

$$I(t, d) = \tilde{I}(\Phi(\mathbf{c}(t, d), \boldsymbol{\xi}), I^{\text{dept}}(\mathbf{c}(t, d), t), t), \quad (17)$$

implying that  $I(t, d)$  depends on  $t$  and  $\mathbf{c}(t, d)$  only. We also use the formulation of

$$I(t, d) = \tilde{I}(\mathbf{c}(t, d), \boldsymbol{\xi}, t) \quad (18)$$

instead of Equation (17) for simplicity.

To facilitate a Markovian representation of the dynamical model, we introduce an auxiliary state variable  $z(t, d)$ , defined by

$$z((t, d) + \mathbf{1}) = \begin{cases} z(t, d) + 1 & \text{if } z(t, d) < t^{\text{Max}} \\ 1 & \text{otherwise} \end{cases} \quad \text{and} \quad z(1, 1) = 1 \quad (19)$$

which can be used to replace the exogenous input of  $t$  in Equation (14), as Equation (19) implies that  $z(t, d) = t$  holds at all times. Substituting  $z(t, d)$  and Equation (18) into Equation (14), we have

$$c_i((t, d) + \mathbf{1}) = \begin{cases} \chi_i(\Phi(\mathbf{c}(t, d), \boldsymbol{\xi}), C_i^+(z(t, d))) & \text{if } i \in \tilde{I}(\mathbf{c}(t, d), \boldsymbol{\xi}, z(t, d)) \\ c_i(t, d) & \text{otherwise} \end{cases}. \quad (20)$$

The dynamics obtained by combining Equations (19) and (20) can be regarded as a Markov chain model whose state is  $(\mathbf{c}(t, d), z(t, d))$ . We also use the following form:

$$\begin{aligned} \mathbf{c}((t, d) + \mathbf{1}) &= \mathbf{F}(\mathbf{c}(t, d), z(t, d), \boldsymbol{\xi}) \\ z((t, d) + \mathbf{1}) &= Z(z(t, d)), \end{aligned} \quad (21)$$

where  $Z(z(t, d))$  and  $\mathbf{F}(\mathbf{c}(t, d), z(t, d), \boldsymbol{\xi})$  are the functions representing the right-hand side of Equations (19) and (20), respectively. Defining the extended state vector by  $\tilde{\mathbf{c}}(t, d) = (\mathbf{c}(t, d), z(t, d))$ , we also have the following form:

$$\tilde{\mathbf{c}}((t, d) + \mathbf{1}) = \tilde{\mathbf{F}}(\tilde{\mathbf{c}}(t, d), \boldsymbol{\xi}), \quad (22)$$

where

$$\tilde{\mathbf{F}}(\tilde{\mathbf{c}}(t, d), \boldsymbol{\xi}) = (\mathbf{F}(\mathbf{c}(t, d), z(t, d), \boldsymbol{\xi}), Z(z(t, d))) \quad (23)$$

is the function representing the transition of the extended state  $\tilde{\mathbf{c}}(t, d)$ . This is further converted to the following transition-matrix form

$$\tilde{\mathbf{q}}((t, d) + \mathbf{1}) = \tilde{\mathbf{P}}\tilde{\mathbf{q}}(t, d), \quad (24)$$

where  $\tilde{\mathbf{q}}(t, d)$  is the probability vector consisting of probabilities of all states, and  $\tilde{\mathbf{P}}$  is the transition matrix determined by Equation (22). Note that the Markov chain model characterised by Equation (24) is not aperiodic owing to the deterministic recurrence formula for  $z(t, d)$  as defined by Equation (19).

## 2.4 Multiple transitions of the Markov-chain dynamical model

Including  $z(t, d)$  in the state vector is beneficial for constructing a Markov chain model including both day-to-day and within-day dynamics in a unified form. However, this causes periodicity in the Markov chain, which prevents the existence of a unique stationary distribution. A simple approach to remove  $z(t, d)$  from the extended state vector is to combine  $t^{\text{Max}}$  times transitions by  $\tilde{\mathbf{F}}$  into a new single transition. This operation always converts  $z(t, d)$  to the same value. Denote the repetition of the operation  $+\mathbf{1}$  by the following form:

$$(t, d) + \mathbf{1} + \dots + \mathbf{1} = (t, d) + \mathbf{1} \times m, \quad (25)$$

where  $m$  is the number of repetitions of the operation  $+\mathbf{1}$ . Then, the  $t^{\text{Max}}$ -times multiple transitions of the Markov chain can be described as

$$\tilde{\mathbf{c}}((t, d) + \mathbf{1} \times t^{\text{Max}}) = \tilde{\mathbf{F}}^{t^{\text{Max}}}(\tilde{\mathbf{c}}(t, d), \boldsymbol{\xi}) \quad (26)$$

From Equation (19), it is apparent that Equation (26) returns the same  $z(t, d)$ . Equation (26) can be further converted to

$$\mathbf{c}((t, d) + \mathbf{1} \times t^{\text{Max}}) = \underbrace{\mathbf{F}(\mathbf{F}(\dots \mathbf{F}(\mathbf{c}(t, d), t) \dots, Z^{t^{\text{Max}}-2}(t)), Z^{t^{\text{Max}}-1}(t))}_{t^{\text{Max}} \text{ times}} \quad (27)$$

Note that  $\xi$  is omitted in Equation (27) for simplicity. Combining the iterated function on the right-hand side as  $\mathbf{F}^+(\mathbf{c}(t, d); t)$ , we have

$$\mathbf{c}(d + 1, t) = \mathbf{F}^+(\mathbf{c}(d, t); t) \quad (28)$$

and the corresponding transition matrix form as

$$\mathbf{q}(d + 1, t) = P(t)\mathbf{q}(d, t). \quad (29)$$

This recurrence formula can be regarded as a Markov-chain-based day-to-day dynamical model, in which the state is given by the decisions of all users at within-day time  $t$  of day  $d$ . Because all users can choose any choices in the transition of  $\mathbf{F}^+$  with a positive probability, the transition is irreducible. Moreover, because the choice model assigns non-zero probability to ‘no change’, the transition is aperiodic. Therefore, this Markov chain has a unique stationary distribution for each  $t$ . We denote such a stationary distribution as  $\mathbf{q}^*(t)$ , which satisfies

$$\mathbf{q}^*(t) = P(t)\mathbf{q}^*(t). \quad (30)$$

Particularly, when we let  $t = t^{\text{Max}}$ ,  $\mathbf{q}^*(t^{\text{Max}})$  is the stationary distribution of travellers’ actual choices that are determined after all travellers depart, i.e. at  $t = t^{\text{Max}}$ .

## 2.5 Conversion of the dynamical framework model to a static-framework model

We now try to convert the proposed Markov-chain model representing the dynamical framework of decision-making into a single Markov-chain model corresponding to the static framework of decision-making (i.e. traditional day-to-day dynamics). We first need to note that this conversion is not possible unless neglecting two important conditions, i.e. the shrinking property of the choice set and the travellers’ lack of ability to update decisions after departure. Therefore, the conversion explained here is not realistic and hence cannot be used for explicit analysis (whether mathematical or numerical). Nevertheless, this hypothetical conversion is useful for understanding properties of the dynamical framework model.

The conversion itself is very easy; let us neglect the dependency of  $t$  on  $\tilde{I}$  defined in Equation (18) and the shrinking property of the choice set. Then, we have

$$c_i((t, d) + \mathbf{1}) = \begin{cases} \chi_i(\Phi(\mathbf{c}(t, d), \xi), C_i) & \text{if } i \in \tilde{I}(\mathbf{c}(t, d)) \\ c_i(t, d) & \text{otherwise} \end{cases}. \quad (31)$$

as a revised dynamical model, which is a Markov chain model because the right-hand side of Equation (31) depends on the state variable  $\mathbf{c}(t, d)$  and constants only.

If we could adopt this conversion, Equation (31) implies that the behaviour of travellers’ adjustment process is identical to that of a standard day-to-day dynamical model by recognising  $(t, d)$  as a sequence of days, i.e. an increment of the decision time in Equation (31) corresponds to an increment of a day in

a standard model. The probability that WDU occurs at each decision time is generally considered to be smaller than the probability that the IDM occurs. In such cases, under the hypothetical situation described above, the presence of the WDU allows travellers to update their choices in a 'gradual' manner rather than the updates by IDM. This consideration implies an important potential role of WDU: when the probability of WDU occurring at each decision time is low, it allows users to change their behaviour gradually, thereby contributing to improving the stability of the system.

Of course, the above discussion ignores important features of the dynamical framework and thus should be regarded only as a rather weak conjecture based on that premise. To determine whether these features actually exist, the only practical method is to conduct numerical simulations, which will be explained in Sections 4 and 5 in the present paper.

### 3 Measures for evaluating stationary distributions of Markov chains

#### 3.1 Outline of the measures

We now introduce measures for assessing properties of the stationary distribution  $\mathbf{q}^*(t)$ . An outline of the core concepts to be used is as follows:

- (a) The *Cesàro mixing time (CeMT)* or its variant *ti-CeMT*, which is an index characterising the **convergence speed towards the stationary distribution**. It is a variant of the Markov chain mixing time (MCMT), which was introduced in Iryo et al. (2024) to assess the convergence speed of day-to-day dynamical models.
- (b) Three indices for characterising **the properties of the stationary distribution**, namely:
  - *Size index* : the standard deviation of the stationary distribution
  - *Instability index* : the index of the directional bias of the day-to-day dynamics
  - *WDU index*: characterises differences between the stationary distributions associated with different decision times
- (c) *The adaptive resilience analysis*, which analyses **the capability of travellers to adapt to changes in the performance of the transport system within a single day**

We also propose a graphical tool that supplements the above measures by facilitating their interpretability.

Owing to the analytical intractability of general Markov processes, we largely have to resort to numerical simulations, specifically Monte Carlo simulations, to obtain the stationary distribution and perform the evaluations by the measures defined on them. The evaluation measures employed in this study are therefore developed so that they are applicable to the assessment of numerical simulation results. However, even with Monte Carlo simulation, we are confronted with the fact that the problem size of the proposed Markov chain model, namely the number of states, is, in general, extremely large. To understand this point, it is important to recognise that an essential component of the transport system considered in this study is that of within-day dynamics, which often involves many departure time options for travellers. For instance, consider 100 travellers choosing one time slot from ten time slots as their departure times. Even

in such a small transport system, the number of states is around 4.27 trillion, which is already infeasible to handle by a Monte Carlo approach, even when travellers are treated as indistinguishable and only aggregated departure-time distributions are counted. As a consequence, even for traffic assignment problems that would generally be regarded as small-scale in a transport science context, treating all states explicitly becomes intractable, even using numerical approaches. Without any particular technique, the direct application of Monte Carlo methods requires an impractically long computational time to obtain results with acceptably low Monte Carlo error.

To ensure that the proposed measures remain computationally tractable for, at least, small- to medium-scale traffic assignment problems, and potentially beyond, specially-designed *aggregation* techniques (Iryo et al., 2024) are adopted. These aggregation methods combine different states, typically those associated with similar properties, into a single state, called the *aggregate state*. This reduces the number of states in the Markov chain. The frequencies of occurrence are then counted based on each aggregated state in Monte Carlo simulations. Note that aggregation is applied only when computing frequencies from the Monte Carlo output; the simulations themselves are performed using the original, unaggregated state representation and unaggregated dynamics that were initially defined on it.

The main improvement in the present paper from the aggregation technique proposed in Iryo et al. (2024) is the retention of the original model's information to the greatest extent possible. While aggregation enables Monte Carlo simulation to be computationally feasible, it simultaneously results in a loss of information about the distributions of the original states prior to aggregation. To alleviate this issue, we propose aggregation approaches in which the loss of information is minimised as far as possible.

In this section, we provide a detailed explanation of the methods introduced above. We first explain the details of the aggregation methods, followed by the definition of the distance between two probability distributions, *TV (total variation) distance*, which is utilised in the calculation processes of the proposed indices. Then, using these tools, we finally explain the details of the measures and definitions of indices, accompanied by corresponding graphical tools, if applicable.

### 3.2 Aggregation with minimal information loss

We first start with an explicit definition of the aggregation approach, following concepts introduced in Iryo et al. (2024). The aggregation, denoted by  $A$ , is defined as a partition of  $C$ . For example, when  $C = \{\mathbf{c}_1, \mathbf{c}_2, \mathbf{c}_3, \mathbf{c}_4, \mathbf{c}_5, \mathbf{c}_6\}$ , the aggregation will be e.g.  $A = \{a_1, a_2, a_3\} = \{\{\mathbf{c}_1, \mathbf{c}_2\}, \{\mathbf{c}_3, \mathbf{c}_4\}, \{\mathbf{c}_5, \mathbf{c}_6\}\}$ , where  $a_i = \{\mathbf{c}_{2i-1}, \mathbf{c}_{2i}\}$  for  $i = 1, 2$  and  $3$ .

The aggregated states can be further aggregated, e.g.  $A^+ = \{a_1^+, a_{23}^+\} = \{\{\mathbf{c}_1, \mathbf{c}_2\}, \{\mathbf{c}_3, \mathbf{c}_4, \mathbf{c}_5, \mathbf{c}_6\}\}$  by merging two or more aggregate states (i.e.  $a_2$  and  $a_3$ ) into a new larger aggregate state (i.e.  $a_{23}^+$ ). When  $A^+$  is the aggregation of  $A$ , we denote this relationship by  $A^+ < A$ . The inequality sign reflects that the number of aggregated states in  $A^+$  is smaller than that in  $A$ . We also define

$$A(a^+) = \{a | a^+ \cap a \neq \emptyset, a \in A\} \quad \forall a^+ \in A^+ \quad (32)$$

to express the set of the aggregated states in  $A$  which are further aggregated to  $a^+ \in A^+$ .

We now introduce a special form of the aggregation based on the number of travellers choosing the same choice. Let us denote the collection of groups of travellers by the set  $G$  and the choice set of group  $g \in G$  by  $C^g$ . Then, we define the vector  $\mathbf{x} = (x_c^g)_{c \in C^g, g \in G}$ , where  $x_c^g$  is the number of travellers in group  $g$  choosing alternative  $c$ . We denote the set of all feasible  $\mathbf{x}$  corresponding to all  $\mathbf{c} \in C$  by  $X$ . We denote by  $\mathbf{x}(d, t)$  the result of the aggregation process applied to  $\mathbf{c}(d, t)$  when it is necessary to indicate

its dependency on  $d$  and  $t$  explicitly. For other forms of aggregations, we use  $\mathbf{y} = (y_a)_{a \in A}$  to denote the number of travellers whose choice belongs to the aggregate state  $a$ .

We consider three aggregation approaches to alleviate the loss of information about the distributions of the original unaggregated states, as enumerated below:

1. aggregations based solely on prior knowledge of the transport system,
2. aggregations using statistical methods aimed at preserving as much of the original information as possible,
3. combinations of both 1 and 2

Approach 1 is the simplest way to aggregate states when we already understand the key influencing factors of travellers' behaviour. For example, if our sole interest is in the average of all travellers' departure times and we have no interest in other characteristics such as the standard deviation, we can simply employ this average to characterise the aggregated states. More specifically, we first define the average departure time as

$$\bar{\tau} = \frac{1}{|I|} \sum_{i \in I} \tau_i \quad (33)$$

and then discretise  $\bar{\tau}$  into equal-width intervals  $\Delta\tau$  by

$$k = \lfloor \bar{\tau} / \Delta\tau \rfloor, \quad (34)$$

where  $k$  constitutes each aggregated state. We now let  $K$  be the set of  $k$ , which represents the aggregation in this form. As far as departure times are lower- and upper-bounded (which is a natural setting in the departure-time choice problems), this operation always leads to a finite number of aggregated states, and its size can be ensured to be practically feasible by employing an appropriate value for  $\Delta\tau$ , say 1 minute if considering a time window of several hours for the morning peak.

Approach 2 aims to achieve data-oriented aggregation when there is no a priori knowledge or preference regarding properties of travellers' behaviour. Methods in this approach include clustering, such as k-means clustering, and dimension reduction techniques, such as UMAP (uniform manifold approximation and projection) and PCA (principal component analysis). These methods can be applied in general cases once we perform the aggregation to vector  $\mathbf{x}$  explained above. As  $\mathbf{x}$  is the vector of integers, computations requested by the distance-based methods, such as k-means and UMAP, are straightforward to apply using standard definitions of distance, such as the Euclidean norm. We can also input  $\mathbf{x}$  directly to PCA. This approach automatically performs the aggregation into a reasonable number of states with minimum loss of information while reducing the number of states.

Approach 3 is a variant of Approach 1, where the parameters used for aggregation are determined using a statistical method. This approach is used when the aggregation approach is determined using a priori knowledge of the system, but when it involves parameters that cannot be identified with such knowledge. We particularly consider the aggregation function that projects  $\mathbf{x} \in X$  onto a lower-dimensional plane, where the function is pre-defined with a few parameters. Detailed steps of this approach are as follows:

1. Define the projection by a multi-dimensional (but lower than the dimension of  $\mathbf{x}$ ) function  $\mathbf{F}^{\text{Proj}}(\mathbf{x}, \boldsymbol{\beta})$ , where  $\boldsymbol{\beta}$  is the vector of the parameters.

2. Then, we set  $\beta$  so that the information ratio is maximised, where the information ratio is defined as the ratio of sum of variances of all components in  $\mathbf{x}$  to that of all components in  $\mathbf{F}^{\text{Proj}}(\mathbf{x}, \beta)$ .
3. The space after the projection, denoted by  $Y$ , is partitioned into discrete aggregate states—for example, by applying a grid system. In the remainder of this paper, we use the term grid instead of partition. Each grid constitutes the aggregate state, and their set is denoted by  $A^{\text{Proj}}$ . We also denote the set of the projected vectors belonging to the grid  $a \in A^{\text{Proj}}$  by  $Y(a)$ .

A representative example arises when the number of travellers choosing different time slots is denoted by  $\mathbf{x}$ , and these are aggregated into three broader time periods, with the boundaries of these periods specified as parameters. Defining the boundaries a priori is not straightforward; for example, we may be able to arbitrarily set them, say as 8 a.m. and 9 a.m., but if the Markov-chain dynamics provides a significant variation before 8 a.m. only, this strategy largely loses information regarding the dynamics. The proposed approach helps identify these boundaries while preserving the variations of the original states.

Each of the three methods described above has its own advantages and disadvantages. Approach 1 requires a prior specification of the characteristics of the transport system to be examined, which is not always straightforward. However, once this is achieved, this approach yields robust and easily interpretable results. Approach 2 is expected to minimise information reduction without prior knowledge, but the interpretability of the results may not be good. Approach 3 is intermediate between these two. We only employ Approaches 1 and 3 in the present study, and these detailed definitions for the case study will be introduced in Section 4.

### 3.3 TV distances

The total variation (TV) distance is introduced to measure the difference between two probability distributions. Let  $\mathbf{p}_1 = (p_1(a))_{a \in A}$  and  $\mathbf{p}_2 = (p_2(a))_{a \in A}$  be two probability distributions of the aggregated states in  $A$ . Then, the TV distance between two distributions is defined as one-half the L1 norm of their difference, namely

$$\|\mathbf{p}_1 - \mathbf{p}_2\|_{\text{TV}} = \frac{1}{2} \sum_{a \in A} |p_1(a) - p_2(a)|. \quad (35)$$

The TV distance is always non-negative and not greater than one.

Iryo et al. (2024) has shown that aggregation, under the definition adopted here, does not increase the TV distance. More specifically, let  $A^+$  be an aggregation of  $A$ , and define the probability distribution of  $A^+$  as

$$p_i^+(a^+) = \sum_{a \in A(a^+)} p_i(a) \quad \forall i \in \{1, 2\}, \quad (36)$$

and define its vector form as  $\mathbf{p}_i^+ = (p_i^+(a^+))_{a^+ \in A^+}$ . Then, the following inequality holds:

$$\|\mathbf{p}_1^+ - \mathbf{p}_2^+\|_{\text{TV}} \leq \|\mathbf{p}_1 - \mathbf{p}_2\|_{\text{TV}}. \quad (37)$$

This implies that aggregation would cause a reduction in the TV distance but never an increase, while Iryo et al. (2024) noted that aggregation does not necessarily significantly reduce the TV distance.

### 3.4 Formulations of measures

We now explain formulations of relevant measures, i.e. (ti-)CeMT, size/instability/WDU indices, and the adaptive resilience analysis. These measures are formulated for a Markov chain model defined by Equation (29). Note that (ti-)CeMT and size/instability indices are separately calculated at specified decision times, as the Markov chain defined by Equation (29) is attributed to the decision time. For these indices, we consider only the Markov chain with  $t = t^{\text{Max}}$ , i.e., the chain representing actual travellers' choices determined at the end of each day.

#### 3.4.1 Cesàro Mixing Time (CeMT)

We first explain the MCMT and its variant, called ti-MCMT, before introducing the Cesàro Mixing Time (CeMT). The original definition of the MCMT is the time it takes for a Markov chain to approach its stationary distribution from any initial state. However, this definition is challenging to apply in Monte Carlo-based numerical simulations for two main reasons: (1) computing the stationary distribution in advance is non-trivial, and (2) running simulations from all possible initial states is virtually impossible. To mitigate these issues, Iryo et al. (2024) introduced a variant of the MCMT, named ti-MCMT ('ti' stands for 'two initial states') as a reasonable alternative to the original MCMT.

The definition of the ti-MCMT is constructed using the TV distances between two Markov chains starting from two different initial states. Let  $\mathbf{p}(d; \mathbf{c})$  be the probability distribution of the Markov chain on day  $d$ , where  $\mathbf{c}$  is the initial state when  $d = 0$ , and let  $\mathbf{c}_1, \mathbf{c}_2 \in C$  are two initial states, where  $\mathbf{c}_1 \neq \mathbf{c}_2$ . Then ti-MCMT, denoted by  $d_{\text{ti}}^{\Theta}(\mathbf{c}_1, \mathbf{c}_2)$  is defined as

$$d_{\text{ti}}^{\Theta}(\mathbf{c}_1, \mathbf{c}_2) = \max \{d \mid \|\mathbf{p}(d; \mathbf{c}_1) - \mathbf{p}(d; \mathbf{c}_2)\|_{\text{TV}} \geq \Theta \}, \quad (38)$$

where  $\Theta$  is a threshold, often defined as 0.25 in the literature (see e.g. Levin and Peres (2017)). The choice of two initial states stipulates the value of the ti-MCMT. It would be better to enumerate several options and choose one that achieves the greatest TV distance, leading to the greatest ti-MCMT, for the conservative assessment of the convergence time.

Then, we introduce the CeMT and ti-CeMT as a variant of the MCMT and ti-MCMT. It is defined as the time it takes for a *temporal average* of a Markov chain to approach its stationary distribution from any initial state. Let  $\bar{\mathbf{p}}(d; \mathbf{c})$  be the temporal average of  $\mathbf{p}(d; \mathbf{c})$  till day  $d$ , namely

$$\bar{\mathbf{p}}(d; \mathbf{c}) = \frac{1}{d} \sum_{d'=1}^d \mathbf{p}(d'; \mathbf{c}). \quad (39)$$

The CeMT is defined as the time when the TV distance between  $\bar{\mathbf{p}}(d; \mathbf{c})$  and the stationary distribution is below the given threshold. We also define the ti-CeMT here, following the definition of the ti-MCMT. Let  $\mathbf{c}_1 \neq \mathbf{c}_2 \in C$  are two initial states. Then, the ti-CeMT is defined as

$$d_{\text{Ce}}^{\Theta}(\mathbf{c}_1, \mathbf{c}_2) = \max \{d \mid \|\bar{\mathbf{p}}(d; \mathbf{c}_1) - \bar{\mathbf{p}}(d; \mathbf{c}_2)\|_{\text{TV}} \geq \Theta \}. \quad (40)$$

For the same reason in the MCMT and ti-MCMT, the ti-CeMT can be a reasonable alternative to the original CeMT, as it does not incur calculations of the stationary distribution and simulations from all possible initial states.

The (ti-)CeMT is particularly useful when the (ti-)MCMT becomes unrealistically large as a result of the strong dominance of stochastic periodicity in the Markov chain rather than random fluctuations. In

such cases, if two initial states are chosen far apart, their trajectories will not overlap until the stochastic fluctuations have spread sufficiently to cover most of the stochastic periodicity. This dispersion process can take an extremely long time when stochastic periodicity is very strong, resulting in an impractically large (ti-)MCMT, which may span, for example, several decades or more. In addition, it should demand more computational time than is reasonable for convergence. Taking the temporal average using Equation (39) significantly mitigates this issue by smoothing out the phase differences between two Markov-chain trajectories.

The (ti-)CeMT is justified when the goal is to assess the long-run average behaviour of the transport system, rather than its performance on any specific day. From a planning perspective, long-term averages often offer more meaningful insights for infrastructure investment or policy evaluation than considering short-term correlations due to the strong stochastic periodicity of the day-to-day dynamics. In addition, the use of (ti-)CeMT makes the computation time practically manageable, especially when the original (ti-)MCMT is prohibitively large due to strong stochastic periodicity. In the present study, our primary objective is to evaluate how the convergence time changes with the introduction of the proposed model, rather than to precisely measure its absolute value. Accordingly, the adoption of (ti-)CeMT is not only practical but also methodologically appropriate for the objectives of this study.

We also utilise the ti-CeMT to determine the sample sequences for calculating indices characterising the properties of the stationary distribution, which will be defined in the subsequent subsections. Using a temporal average for calculating the indices in the stationary distribution is adopted by the Ergodic Theorem (see e.g. Levin and Peres (2017), Appendix C).

In the present paper, we employ an aggregation technique (specifically, Aggregation 3) when numerically computing the (ti-)CeMT, as the number of unaggregated states can be extremely large. Inequality (37) ensures that the TV distance does not increase as a result of aggregation, which in turn implies that the (ti-)CeMT does not increase. The discussion immediately following this inequality also suggests that aggregation does not necessarily lead to a significant reduction in the (ti-)CeMT.

### 3.4.2 Three indices for characterising the properties of the stationary distribution

The **size index**, denoted by  $\zeta^{\text{Size}}$ , is defined by the following formula:

$$\zeta^{\text{Size}} = \sqrt{\sum_{\mathbf{x} \in X} p^*(\mathbf{x}) |\mathbf{x} - \bar{\mathbf{x}}|^2} \quad (41)$$

where  $p^*(\mathbf{x})$  is the probability that  $\mathbf{x}$  occurs in the stationary distribution for  $t = t^{\text{Max}}$ , and

$$\bar{\mathbf{x}} = \sum_{\mathbf{x} \in X} p^*(\mathbf{x}) \mathbf{x}. \quad (42)$$

Note that the Euclidean norm is adopted to calculate the distance in Equation (41). In the graphical representation of the size index, the Euclidean norm between  $\mathbf{x}(t^{\text{Max}}, d)$  and  $\bar{\mathbf{x}}$ , denoted by

$$d^{\text{Em}}(d) = |\mathbf{x}(t^{\text{Max}}, d) - \bar{\mathbf{x}}|, \quad (43)$$

and called *Euclidean norm from the mean*, is utilised to depict the time-dependent nature of the day-to-day dynamics of a chain by letting  $d$  be sufficiently large so that the state is in the stationary distribution. This time series, plotted over days, reflects not only the size index (i.e. the magnitude of deviations from the

mean) but also the properties of the system's dynamical behaviour, namely whether random fluctuations or stochastic periodicity are dominant.

The **instability index** describes how far the direction of the dynamics from a certain aggregated state is biased in the stationary distribution. This index is defined by utilising the aggregation of Approach 3. Let  $\mathbf{y}(d) \in Y$  be the vector projected from  $\mathbf{c}(t^{\text{Max}}, d)$  onto space  $Y$  through the aggregation to  $X$  and the projection function  $\mathbf{F}^{\text{Proj}}(\mathbf{x}, \boldsymbol{\beta})$ . Then, the motion vector  $\Delta\mathbf{y}(d)$  is defined as

$$\Delta\mathbf{y}(d) = \mathbf{y}(d+1) - \mathbf{y}(d), \quad (44)$$

which leads to the definition of the average motion of each grid as

$$\bar{\mathbf{y}}(a) = \mathbb{E}(\Delta\mathbf{y}(d) | \mathbf{y}(d) \in Y(a)) \quad \forall a \in A^{\text{Proj}}, \quad (45)$$

where  $\mathbf{y}(d)$  and  $\mathbf{y}(d+1)$  follow the stationary distribution.

While the motion vectors and their average are useful to identify the 'speed' of the behavioural change *per day*, we need to be aware that this speed primarily depends on the number of travellers revising their choices on a day, and then secondary depends on how the motion of the system is biased in each grid. We therefore normalise the speed vector by the average number of travellers revising choices to extract information on the bias of motion. Let  $\bar{n}_{\text{revise}}$  be the average number of travellers revising choices per day, which will be estimated by the Monte Carlo simulation. Then we define

$$\Delta\mathbf{v}^{\text{Inst}}(a) = \frac{1}{\bar{n}_{\text{revise}}} \mathbb{E}(\Delta\mathbf{y}(d) | \mathbf{y}(d) \in Y(a)) \quad \forall a \in A^{\text{Proj}}, \quad (46)$$

and the instability index as follows:

$$\zeta^{\text{Inst}} = \sum_{a \in A^{\text{Proj}}} p^*(a) |\Delta\mathbf{v}^{\text{Inst}}(a)| \quad (47)$$

where  $p^*(a)$  is the probability of  $\mathbf{y}(d) \in Y(a)$  in the stationary distribution. Depicting the average motion on the grid using arrows is adopted as a graphical tool for the instability index.

We finally define the **WDU index** by adopting Approach 1 aggregation, in which the average-departure-time-based aggregation specified by Equation (34) is used. Let  $p^*(k, t)$  be the probability distribution of  $k$  in the stationary distribution of decision time  $t$ . Then, we define the WDU index, denoted by  $\zeta^{\text{WDU}}$ , as the average of the TV distances between two adjacent decision times, namely

$$\zeta^{\text{WDU}} = \frac{1}{2} \sum_{t=1}^{t^{\text{Max}}-1} \sum_{k \in K} |p^*(k, t) - p^*(k, t+1)|. \quad (48)$$

$\zeta^{\text{WDU}} = 0$  if the stationary distributions over  $K$  are identical for all decision times, implying that the within-day decision-making does not affect the aggregated travellers' behaviour characterised by  $p^*(k, t)$ . Conversely, if we find  $\zeta^{\text{WDU}}$  is larger, the within-day decision-making has a large impact on their behaviour. The graphical representation of  $p^*(k, t)$  may be performed by drawing its heat map on the  $k$ - $t$  plane.

### 3.4.3 Adaptive resilience analysis

The adaptive resilience analysis evaluates how travellers' choices and the LOS adapt to new performance parameters of the transport system (e.g., traffic capacity). In this analysis, we consider a situation in

which the performance of the transport system changes suddenly at the beginning of the given day without any prior announcement to travellers. We then examine, through the WDU process, the extent to which users' behaviour adapts to the new situation within the same day when the performance change occurs. Specifically, we adopt the following process:

1. A single day is sampled from the steady state.
2. Immediately after the IDM on that day is completed, the transport system performance parameter  $\xi$  provided to the OTIS is updated to a new value.
3. If necessary, the model determining which users perform WDU at each decision time (i.e., the model for determining  $I(t, d)$ ) is updated from its normal setting to one that reflects travellers' changes of information collection behaviour under the performance change.
4. Based on the results of users' WDU, we obtain the changes in their choices and, consequently, the changes in LOS at the end of the day.
5. Separately, the steady-state distribution based on the new  $\xi$  is computed.
6. By comparing this with the results from steps 4 and 5, we evaluate the extent to which users' behaviour and the LOS have approached their steady-state values within a single day.

The comparison in Process 6 is made in a qualitative or quantitative manner, or both. The TV distance with an appropriate aggregation can be used for quantitative assessment.

The most distinctive feature of this analysis is that it examines the system's adaptive capacity over a single day immediately following a performance change. In traditional static-framework day-to-day dynamics, it is possible to investigate the daily-based adaptivity, namely, how many days it takes for users' behaviour to adapt to a new state after a change in performance. Such analyses are effective when the change in performance persists over the long term (e.g., capacity reductions due to long-term maintenance works). However, this approach is not applicable to performance changes that occur only on a specific day and return to normal by the following day, such as those caused by traffic accidents or adverse weather. By explicitly modelling WDU, the proposed method enables the evaluation of resilience to such one-day incidents, which are expected to occur more frequently in practice. Note that the timing at which the new model parameter is given to the OTIS may be changed depending on scenarios, e.g. it can be later for an accident, and may be earlier than IDM for adverse weather that cannot be forecasted in advance. These details can be incorporated in the proposed process, while we will fix this timing as indicated in the above process in the present study.

## 4 Numerical assessments of the impacts of the dynamical framework

### 4.1 Scenario setting

We performed numerical analyses to assess the impact of the within-day decision-making. We selected Vickrey's departure time choice problem for the numerical analyses. There are two main reasons for this selection. First, this problem is inherently dynamic, as it involves the departure time choices, and is well

aligned with the dynamical framework incorporated in the proposed model. As discussed in Section 2, the model categorises users' choices into two components: departure times ( $\tau_i$ ) as the primary component, and other attributes, such as route choices ( $r_i$ ), as secondary components. Given this formulation, it is particularly appropriate to adopt case studies that focus on departure time choices. Second, past studies have shown that the day-to-day dynamics of Vickrey's departure time problem do not necessarily converge to an equilibrium, and that the equilibrium itself may be unstable (see, e.g. Iryo (2008), Guo et al. (2018), Iryo (2019), Lamotte and Geroliminis (2021), and Satsukawa et al. (2024)). These non-convergent and unstable properties necessitate a dynamical analysis of the model rather than a static equilibrium analysis. Therefore, investigating this type of problem using the proposed model is also valuable for advancing our understanding of the underlying mechanisms of such problems.

The detailed settings are as follows. We consider a single-road network consisting of a single origin-destination pair and one capacitated bottleneck between them. All travellers have to travel from the origin to the destination using this road by car without sharing a ride. They do not have any other choices, such as using an alternative route/mode or stopping travelling. There may be delays at the bottleneck if the incoming traffic flow exceeds its capacity. The point queue model is used to calculate the delay at the bottleneck. The number of travellers on this road is 1,800. The capacity of the bottleneck is 1,800 vehicles per hour.

Travellers choose their incoming times to the bottleneck. As we adopt the point queue model, travellers depart from the bottleneck immediately upon arrival when no queue is present; that is, no free-flow travel time at the bottleneck is considered. We also assume that free-flow travel time from the origin to the bottleneck is the same for all travellers and constant. This assumption allows us to let this free-flow travel time be zero because we consider the OTIS as the information provision mechanism. With OTIS, travellers can accurately know the LOS immediately after they fix their decisions and depart, before they actually arrive at the bottleneck and form a queue. The free-flow travel time does not affect travellers' behaviour at all in this setting. We divide the study period of the incoming time to the bottleneck, which is two hours long, into 120 time slots, where each time slot is one minute. Travellers are assumed to choose either one of these slots. We hereafter assume that traveller  $i$ 's departure time slot from the origin, denoted by  $\tau_i \in T = \{1, \dots, t^{\text{Max}}\}$ , where  $t^{\text{Max}} = 120$ , is equal to their arrival time at the bottleneck. The  $i$ th time slot corresponds to the period between  $i - 1$  minutes and  $i$  minutes from the beginning of the study period. We also assume that the free-flow travel time from the bottleneck to the destination is zero without loss of generality.

Travellers are homogeneous and have the same travel preferences. Their travel cost is the sum of the delay at the bottleneck and the schedule cost at the destination. The schedule cost is  $0.6\Delta T_s$  for early arrivals and  $6\Delta T_s$  for late arrivals, where  $\Delta T_s$  is the difference between the desired arrival time and the actual arrival time. Their desired arrival time is 80 minutes after the start of the study period.

All travellers make the IDM every day with probability  $p^I$ . They also make the WDU at every time slot with probability  $p^W$  unless they depart. Note that  $p^W$  does not depend on whether travellers have already performed the WDU on the same day or not, so they may make multiple WDU before their departures.

The error term  $\varepsilon_{ci}(t, d)$  is assumed to follow the normal distribution, whose standard deviation is denoted by  $\sigma$ . To obtain the random values correlated over different departure time choices in the Monte Carlo simulation, we generated correlated Gaussian random vectors by building a covariance matrix in which the correlation between two elements decreases exponentially with their index distance. Cholesky decomposition was then applied to the matrix, and standard normal vectors were transformed to produce the correlation. The correlation coefficient is denoted by  $\rho$ .

We now have four system parameters of the case study, namely  $p^I$ ,  $p^W$ ,  $\sigma$ , and  $\rho$ . We adopted all the combinations of these parameters from the following values:

- $p^I$ : 0.002, 0.005, 0.01, 0.02, 0.05, 0.1
- $p^W$ : 0.0, 0.0001, 0.0002, 0.0005, 0.001, 0.002, 0.005, 0.01
- $\sigma$ :  $10^{-10}$ , 0.01, 0.1, 0.2, 0.5, 1.0 (min)
- $\rho$ : 0.0 (no correlation) and 0.9.

The number of combinations of these parameters is 576.

We adopted Approaches 1 and 3 for the aggregation. For Approach 1, we adopted  $\Delta\tau = 0.01$ . For Approach 3, let us denote the number of travellers choosing  $\tau$  th incoming time slot by  $x(\tau, t, d)$  and let  $\mathbf{x}(t, d) = (x(\tau, t, d))_{\tau \in T}$ . We define the projection function with parameters  $n_1$  and  $n_2$  as follows:

$$y_1(t, d) = \sum_{\tau=1}^{n_1} x(\tau, t, d), \quad y_2(t, d) = \sum_{\tau=n_1+1}^{n_2} x(\tau, t, d), \quad y_3(t, d) = \sum_{\tau=n_2+1}^{120} x(\tau, t, d). \quad (49)$$

We also refer to the first, second, and the third time period as *earliest*, *middle*, and *latest* time period, respectively. We do not use  $y_3(t, d)$  because  $y_1(t, d) + y_2(t, d) + y_3(t, d) = 1800$  at all times, and hence the result of this aggregation process can be plotted to  $(y_1(t, d), y_2(t, d))$  on the two-dimensional plane. We further disaggregate  $y_1(t, d)$  and  $y_2(t, d)$  using a grid system with intervals 0–99, 100–199, ..., and 1700–1800; note that the last interval is one unit larger than the others.

The Monte Carlo simulations were performed to obtain samples for estimations of probability distributions and indices defined in Section 3. The number of chains was 24 for each system parameter set, which are further classified into two groups (each consisting of 12 chains), where every traveller chooses either the first time slot or the 51st time slot (i.e.  $\tau_i = 1$  or  $\tau_i = 51$  for all  $i \in I$ ) in the initial state of the Markov chain. We define the term *initial time slot* as the time slot chosen by each traveller at the initial state. The length of the chain (i.e. how many days the Monte Carlo simulation was carried out) was determined so that its temporal mean sufficiently converges to the stationary distribution. Its detailed procedure was as follows:

1. Initial calculation: After performing a preliminary calculation for a few parameter sets, a rough estimation of the chain lengths was made. Iryo et al. (2024) has shown that the MCMT is proportional to the revision probability, which corresponds to  $p^I$  and  $p^W$  in the present study. We incorporated this property to determine the initial lengths.
2. Determination of  $n_1, n_2$  for the aggregation: Using the chains calculated at Step 1,  $n_1, n_2$  were determined so that the sum of the variances of  $(y_1(t, d), y_2(t, d), y_3(t, d))$  is maximised. We adopted a common pair of values for  $(n_1, n_2)$  for all parameter settings by the following steps: (1) For each chain of each parameter set,  $n_1$  and  $n_2$  are adjusted individually to calculate the sum of variances of  $y_1, y_2$ , and  $y_3$ , and the maximum sum over all  $n_1, n_2$  combinations is identified. (2) Then, a common pair of  $n_1$  and  $n_2$  is chosen for all cases to maximise the minimum ratio between each case's variance sum (under this common pair) and the previously identified maximum sum. By this process, the selected  $n_1$  and  $n_2$  were 49 and 68, respectively.

3. Determination of chain lengths: Using the aggregation, we calculated the ti-CeMT with threshold 0.025 (ten times smaller than the typical threshold 0.25), i.e.  $d_{Ce}^{0.025}(\mathbf{c}_1, \mathbf{c}_2)$ , where the initial time slot is 1 for  $\mathbf{c}_1$  and 51 for  $\mathbf{c}_2$ , respectively. We adopted a chain length two times longer than this, and consider the temporal mean of the latter half represents the stationary distribution. The latter half of the chain is referred to as the *converged chain*.

All indices were calculated using 24 samples of chains for each parameter set.

## 4.2 Graphical representation of key cases

We illustrate the properties of the dynamics and the stationary distributions of the proposed model using the graphical tools proposed in Section 3. The impacts of the within-day decision-making on the day-to-day dynamics are also qualitatively assessed in this section. More quantitative analyses will follow in the next section.

We first show the graphs of the incoming traffic flow (i.e.  $x(\tau; t, d)$ ) and delays at the bottleneck) in Figures 3 and 4. The result indicates an important impact of within-day decision-making, namely the suppression of fluctuations in flow and delay patterns in the stationary distribution. This point will be further investigated using the proposed indices, not only for this case but also for other parameter cases.

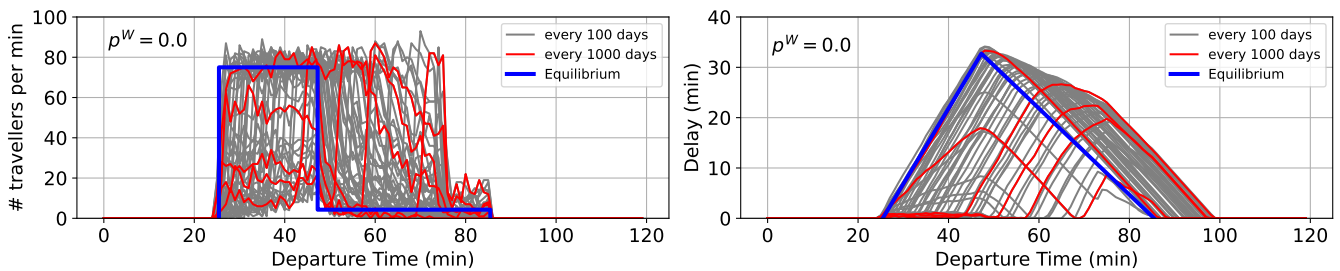


Figure 3: Incoming flow (left) and delay (right) profile; No WDU (i.e.  $p^W = 0.0$ ),  $(p^I, \sigma, \rho) = (0.01, 0.1, 0.0)$ , initial time slot = 1

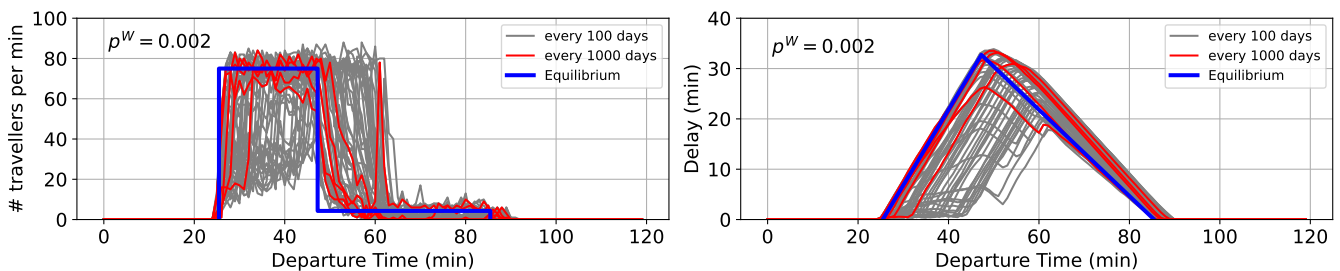


Figure 4: Incoming flow (left) and delay (right) profile;  $p^W=0.002$ ,  $(p^I, \sigma, \rho) = (0.01, 0.1, 0.0, 0)$ , initial time slot = 1

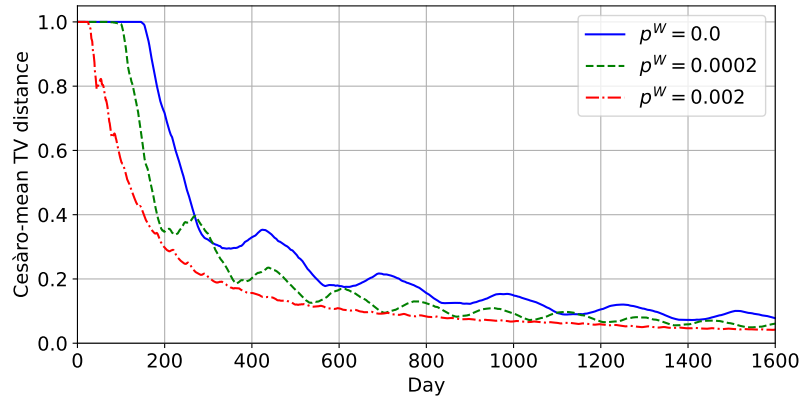


Figure 5: Cesàro-mean based TV distances between two chains starting from initial time slot 1 and 51.

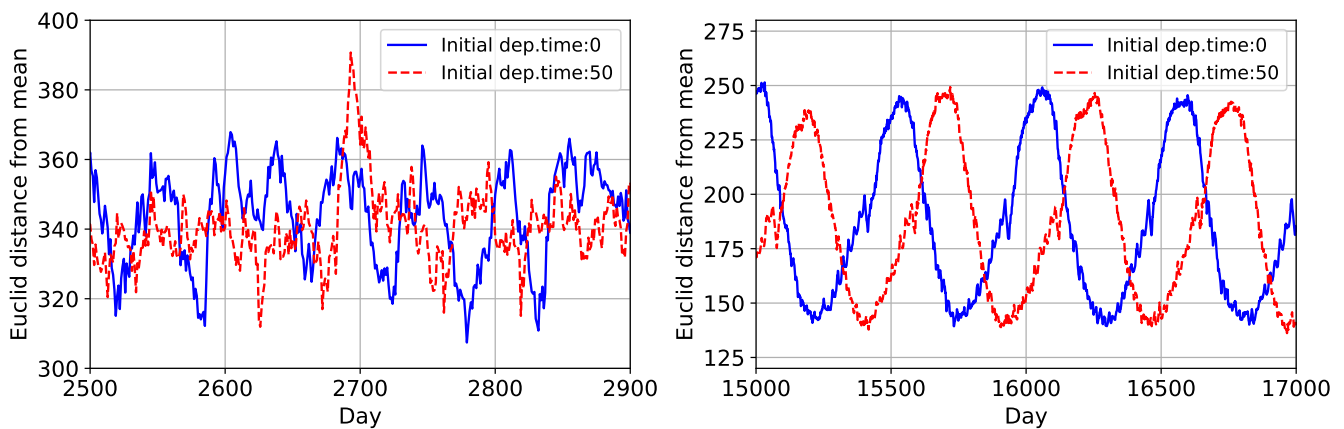


Figure 6: Day-to-day changes of Euclidean norm from the mean ( $d^{\text{EM}}(d)$ ) in the converged chains; left:  $p^{\text{I}}=0.1$ , right:  $p^{\text{I}} = 0.01$ . Other parameters:  $(p^{\text{W}}, \sigma, \rho) = (0.02, 0.5, 0.0)$

Next, in Figure 5, we observe changes in the Cesàro-mean based TV distance between two chains starting from different initial states, where the initial time slot is either 1 or 51. Although we observe mild oscillations, the TV distances tend to decrease with respect to the day. This result suggests convergence of the time-averaged probability distribution within the proposed Markov process.

We also show the day-to-day changes of the Euclidean norm from the mean in the stationary distribution in Figure 6. More stochastic fluctuation was observed in  $p^{\text{I}} = 0.1$ , while strong stochastic periodicity, exhibiting seemingly cyclic behaviour, was observed for a smaller  $p^{\text{I}}$  ( $=0.01$ ). Another implication of the result for  $p^{\text{I}} = 0.01$  is that the effect of the initial state strongly lasts for many days. It can lead to an extremely large MCMT; the chains would virtually not converge to the stationary distribution within a reasonable number of days. This result supports the use of the CeMT instead of the MCMT for assessing the convergence speed.

To visually understand the instability property of the dynamics, we visualise the planar motion of the state using the  $\Delta \mathbf{v}^{\text{Inst}}(a)$ . Figures 7 (without WDU) and 8 (with WDU) show the results. In these figures, the arrows indicate  $\Delta \mathbf{v}^{\text{Inst}}(a)$  in each grid  $a$ , and the darkness of each grid shows its aggregated probability in the stationary distribution. The area surrounded by the blue lines is the feasible area. The vertical and horizontal axes indicate the number of travellers in the early and middle time periods, respectively. When

the number of travellers in the latest time period is zero, the state remains in the vicinity of the diagonal line; when this number is greater than zero, the state approaches the bottom-left corner of the feasible area.

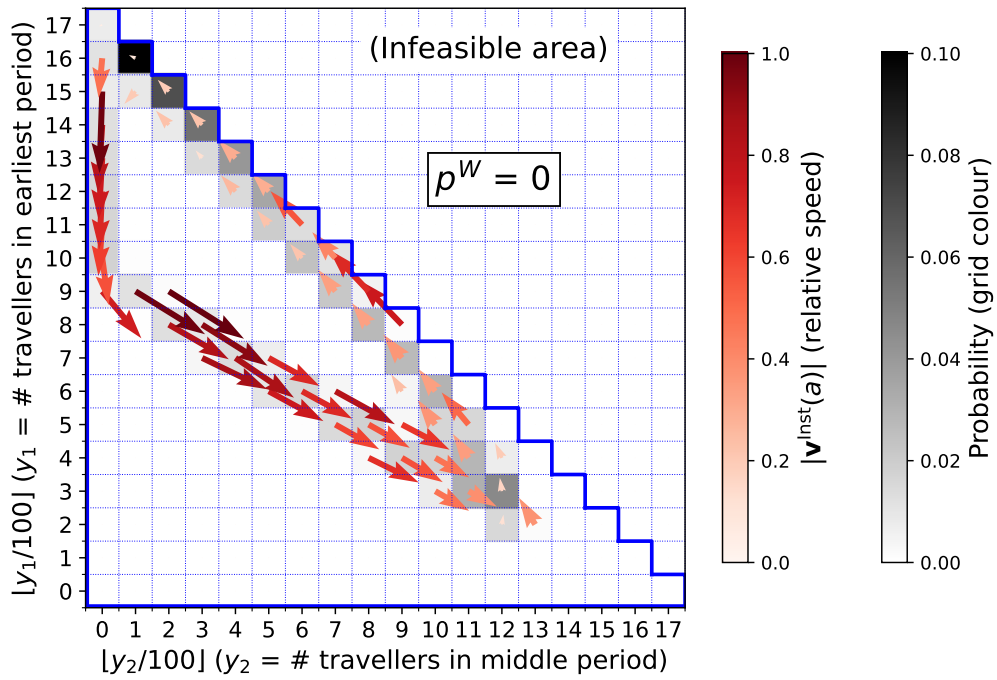


Figure 7: Planar motion of the dynamics by  $\Delta \mathbf{v}^{Inst}(a)$  in the converged chain (without-WDU case).  $(p^I, p^W, \sigma, \rho) = (0.01, 0.0, 0.01, 0.0)$ ; initial time slot = 1

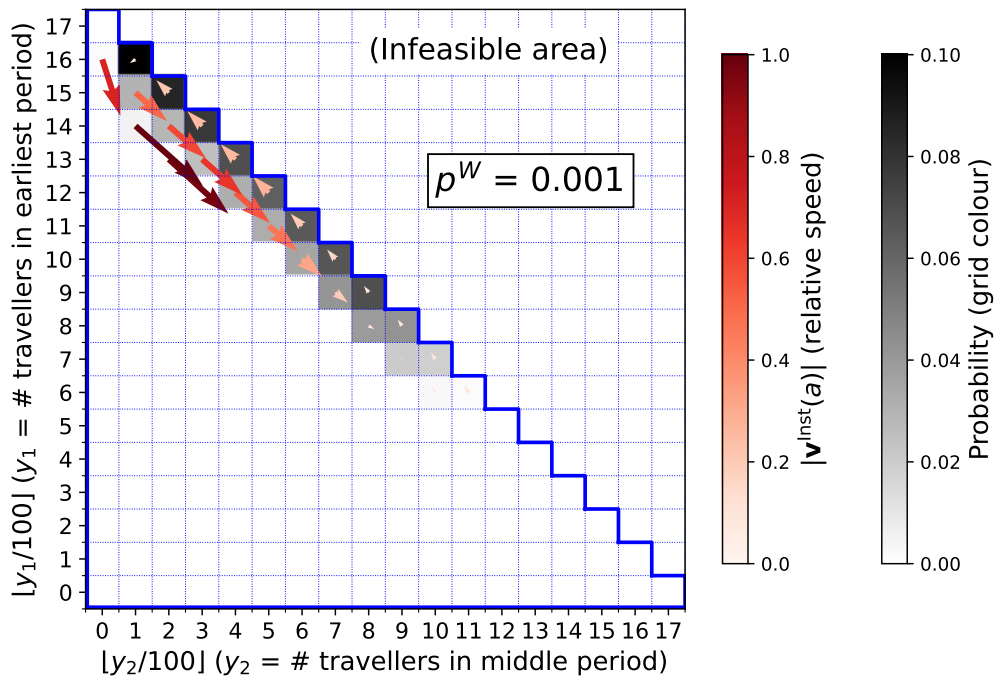


Figure 8: Planar motion of the dynamics by  $\Delta \mathbf{v}^{Inst}(a)$  in the converged chain (with-WDU case).  $(p^I, p^W, \sigma, \rho) = (0.01, 0.001, 0.01, 0.0)$ ; initial time slot = 1

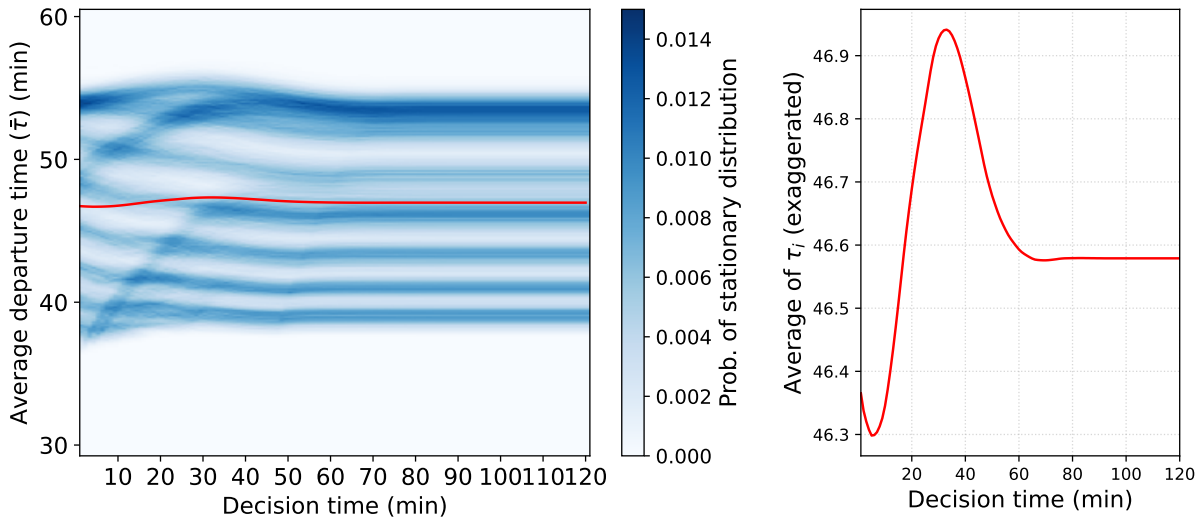


Figure 9: Stationary distribution of  $\bar{\tau}$  with respect to decision time. The red-line plot is the average of the distribution at each decision time  $t$ . The right panel is an exaggerated view of the red plot.

The comparison of the results of these two figures clearly depicts how the dynamics of user departure time choices in the present setting change by introducing the dynamical decision-making framework. In the without-WDU case, we observe strong ‘flow’ in the interior of the feasible area. This motion reflects a strong aggregate tendency of travellers to shift first towards the latest time period, then towards the middle period, and finally back to the earliest period. Such a prominent property is not found in the with-WDU case; the milder movements can be seen on the diagonal line only, implying that most travellers do not choose the latest time period and switch their departure times within the early and middle time slots only.

Finally, we show the WDU property in Figure 9, which indicates the probability distribution of the average departure time at each decision time, namely  $\bar{\tau}(t, d)$ , sampled from the converged chains. It indicates that the probability distribution of  $\bar{\tau}(t, d)$  changes over the decision time  $t$  when it is earlier, then converges to the distribution of  $\bar{\tau}(t^{\text{Max}}, d)$ , which is the average of departure times that travellers have actually chosen. The red line indicates the average of  $\bar{\tau}(t, d)$  at each  $t$ , also reflecting its change over  $t$ . This result suggests that, even in the stationary distribution, travellers may change their departure time within a day before they depart by the WDU process. This observation suggests that the WDU plays an important role not only in the process of convergence to a stationary state, but also in maintaining it.

The main finding from the qualitative assessments using graphical tools is that oscillations clearly appear in the day-to-day dynamics resulting from the combination of the departure time choice problem and the proposed day-to-day dynamics, regardless of whether the WDU process is incorporated. More importantly, we found that *the WDU suppresses these oscillations in the day-to-day dynamics*, thereby making the system more stable. We also see that the time-averaged TV distance decreases with respect to day, and the values of the CeMT are reasonable, at least for the cases shown in 5. These properties will be further investigated in a more quantitative way in the next subsection.

### 4.3 Quantitative analysis of the indices

In this section, we conduct a quantitative analysis of the following indices: CeMT,  $\zeta^{\text{Size}}$ ,  $\zeta^{\text{Inst}}$ , and  $\zeta^{\text{WDU}}$ . The objective is to elaborate on the qualitative insights obtained from the selected cases in the previous

section. This study aims to examine how each index depends on the model parameters by visualising their behaviours without employing any specific statistical models. However, since we consider four parameters —  $p^I$ ,  $p^W$ ,  $\sigma$ , and  $\rho$  — it is not straightforward to represent this dependency in a two-dimensional space. To address this limitation, we adopt the following visualisation strategy:

1. Scatter plots are used for observing variations with respect to error terms. Since  $\rho$  takes only two values (0.0 and 0.9), the values of each index under  $\rho = 0.0$  are plotted on the x-axis, and those under  $\rho = 0.9$  on the y-axis. For  $\sigma$ , which has six values, scatter plots are constructed by placing one value of  $\sigma$  on the x-axis and the remaining values on the y-axis. This method is applied to all indices except  $\zeta^{WDU}$ .
2. To observe variations with respect to  $p^I$  and  $p^W$ , heatmaps are employed with  $p^W$  on the horizontal axis and  $p^I$  on the vertical axis for selected combinations of  $\rho$  and  $\sigma$ . Understanding how the indices change with respect to  $p^I$  and  $p^W$  is central to this study; this method enables a detailed and interpretable representation of such variations.

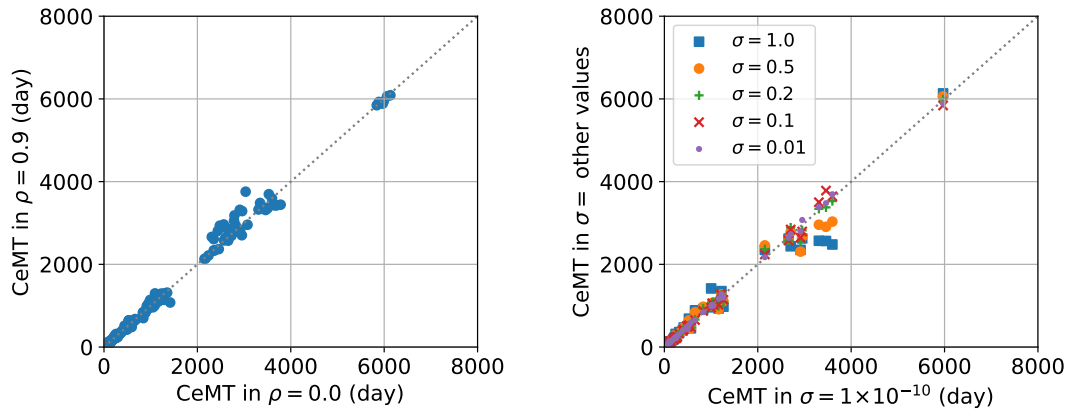


Figure 10: Comparison of CeMT. Each plot indicates the CeMTs of  $\rho = 0.0$  and 0.9 with the same  $p^I, p^W, \sigma$  on the left panel. Each plot indicates the CeMTs of different  $\sigma$  with the same  $p^I, p^W, \rho$  on the right panel.

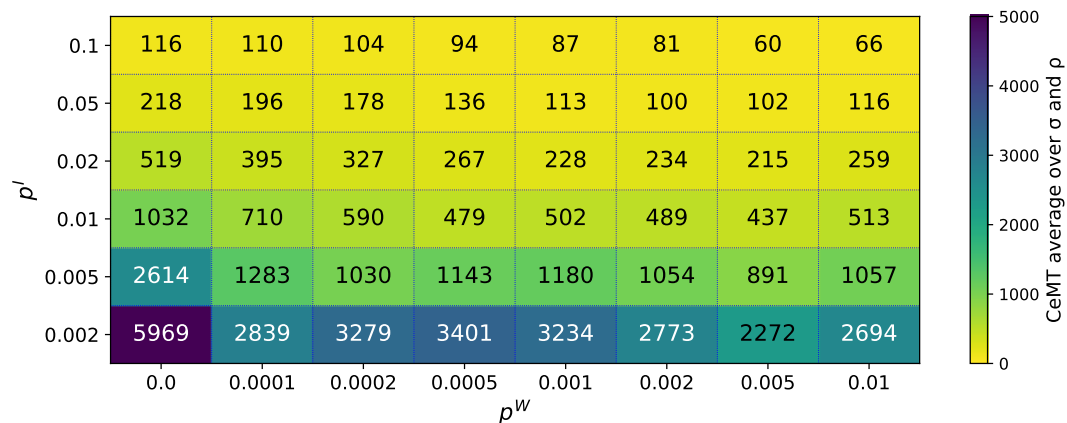


Figure 11: Average of CeMT over all  $\sigma$  and  $\rho$  w.r.t.  $p^I$  and  $p^W$

We first conduct an analysis of the CeMT. Figure 10 contains the scatter plots for observing variations with respect to error terms. The left panel compares the variations with respect to  $\rho$ , and the right panel compares them with respect to  $\sigma$ . We can observe that changing  $\rho$  and  $\sigma$  does not cause any significant change in the CeMT. We also observe variations with respect to  $p^I$  and  $p^W$  using Figure 11. Because the differences in  $\rho$  and  $\sigma$  do not make a significant impact on the CeMT, we took the averages of the CeMT over all combinations of  $\rho$  and  $\sigma$  for each  $p^I$  and  $p^W$ , and have depicted them in this figure. The results suggest that the CeMT depends significantly on  $p^I$ ; specifically, the CeMT becomes approximately five to ten times greater when  $p^I$  decreases by a factor of ten. This dependency is easy to interpret: a smaller  $p^I$  means fewer travellers revise their decisions each day, resulting in a longer convergence time. The CeMT also depends on  $p^W$ , but this dependency is milder compared to that of  $p^I$ .

Next, we analyse how the size index  $\zeta^{Size}$  changes over different parameter settings. Figure 12 contains the scatter plots for observing variations with respect to error terms. In the left panel, we observe that changes in  $\rho$  do not significantly affect  $\zeta^{Size}$ , except for a general trend where  $\zeta^{Size}$  values for  $\rho = 0.9$  tend to be smaller than those for  $\rho = 0.0$ , aside from a few outliers. On the other hand, changes in  $\sigma$  give systematic differences in  $\zeta^{Size}$  as shown in the right panel of the figure. We can read from this figure that, as a general trend, the variation in  $\zeta^{Size}$  across different parameter settings decreases as  $\sigma$  increases. This result would suggest that the error term of the utility function has two roles. The first is to simply add random errors to the solution, thereby increasing  $\zeta^{Size}$ . The second is to suppress the size of stochastically periodic trends, thereby reducing  $\zeta^{Size}$ . Figures 13 and 14 show how  $\zeta^{Size}$  depends on  $p^I$  and  $p^W$  in two cases, i.e.  $(\sigma, \rho) = (0.01, 0.0)$  and  $(1.0, 0.0)$ .

$\zeta^{Size}$  becomes greater with respect to  $p^I$ . This tendency is easy to understand because a larger  $p^I$  implies greater changes in travellers' choices on a single day, while a smaller  $p^I$  implies fewer changes per day, leading to smoother system dynamics. On the other hand, the changes seen in  $\zeta^{Size}$  are not monotonic with respect to  $p^W$  for most  $p^I$ . It means that there is apparently an 'optimal'  $p^W$  that yields the smallest  $\zeta^{Size}$  for any given  $p^I$ . This point would imply two potential roles of the WDU, namely, in suppressing the oscillation if a moderate value of  $p^W$  is assumed, while also increasing the size of the oscillation when  $p^W$  is greater. The latter effect can be considered as the same effect made by a greater  $p^I$ . Note that  $p^W$  is defined as a probability that each traveller performs the WDU in *every single time slot*, so  $p^W = 0.01$  does not necessarily imply a small probability. For example, in the cases shown in Figures 3 and 4, in which travellers' departure times are not earlier than 20 mins before the study period starts, they perform the WDM at least once with probability  $1 - 0.99^{20} \simeq 0.18$ .

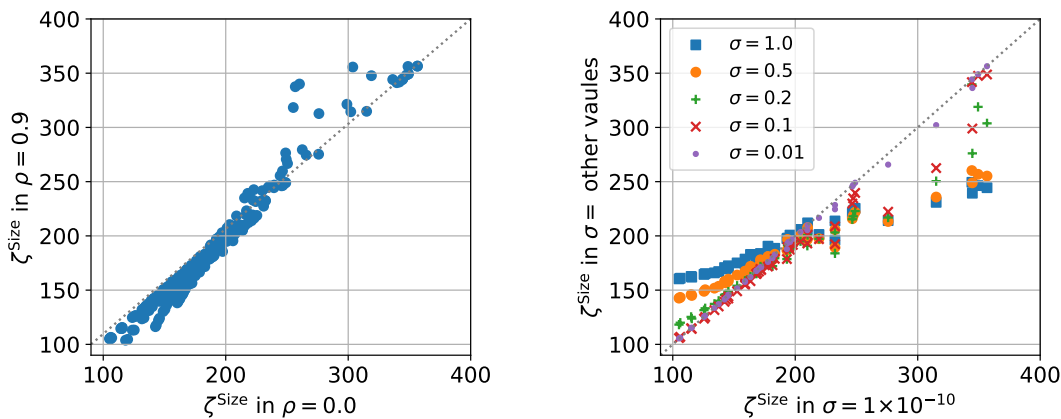


Figure 12: Comparison of  $\zeta^{Size}$ . Each plot indicates the  $\zeta^{Size}$  of  $\rho = 0.0$  and  $0.9$  with the same  $p^I, p^W, \sigma$  on the left panel. Each plot indicates the  $\zeta^{Size}$  of different  $\sigma$  with the same  $p^I, p^W, \rho$  on the right panel.

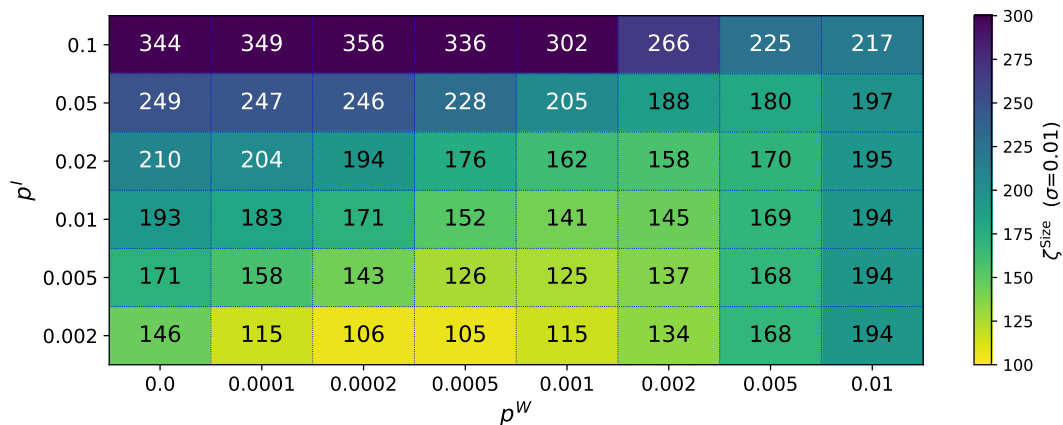


Figure 13:  $\zeta^{\text{Size}}$  w.r.t.  $p^I$  and  $p^W$  where  $\sigma=0.01$  and  $\rho=0$

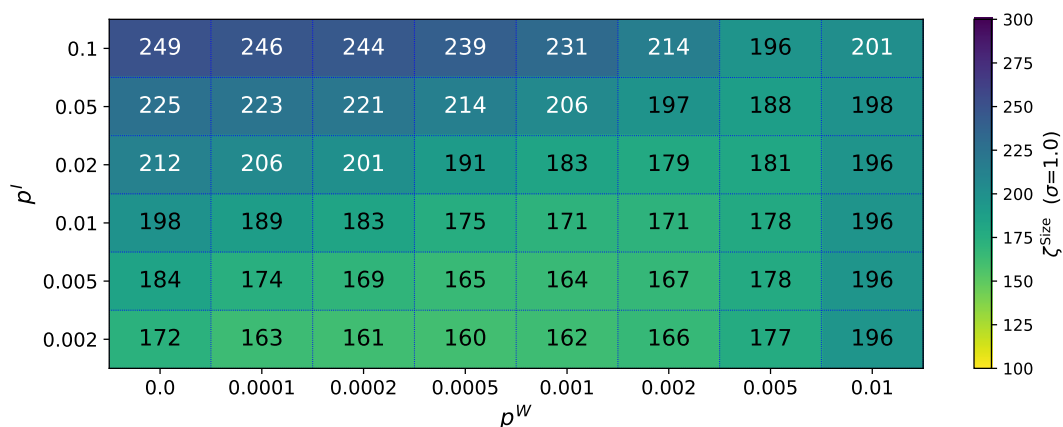


Figure 14:  $\zeta^{\text{Size}}$  w.r.t.  $p^I$  and  $p^W$  where  $\sigma=1.0$  and  $\rho=0$

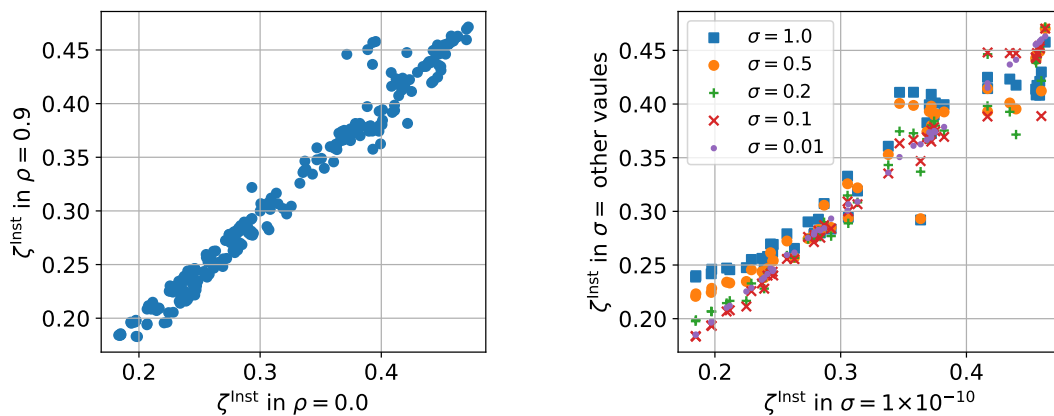


Figure 15: Comparison of  $\zeta^{\text{Inst}}$ . Each plot indicates the  $\zeta^{\text{Inst}}$  of  $\rho = 0.0$  and  $0.9$  with the same  $p^I, p^W, \sigma$  on the left panel. Each plot indicates the  $\zeta^{\text{Inst}}$  of different  $\sigma$  with the same  $p^I, p^W, \rho$  on the right panel.

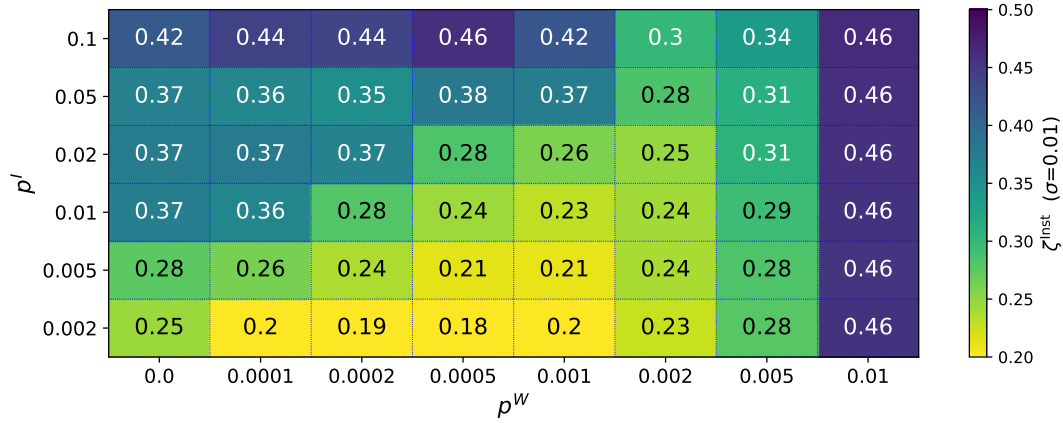


Figure 16:  $\zeta^{\text{Inst}}$  w.r.t.  $p^I$  and  $p^W$  where  $\sigma=0.01$  and  $\rho=0$



Figure 17:  $\zeta^{\text{Inst}}$  w.r.t.  $p^I$  and  $p^W$  where  $\sigma=1.0$  and  $\rho=0$

We also examined changes in the instability index  $\zeta^{\text{Inst}}$  over different parameter settings. The procedure adopted for the comparisons is exactly the same as for  $\zeta^{\text{Size}}$ . Figure 15 is for the comparison by different  $\rho$  and  $\sigma$ , and Figures 16 (where  $\sigma = 0.01$  and  $\rho = 0$ ) and 17 (where  $\sigma = 1.0$  and  $\rho = 0$ ) are for the comparisons by different  $p^W$  and  $p^I$ . We can observe the tendencies that are similar to the size index case, namely (1)  $\zeta^{\text{Inst}}$  for  $\rho = 0.9$  are slightly smaller than for  $\rho = 0.0$  overall, (2) the variation in  $\zeta^{\text{Inst}}$  between different parameters decreases as  $\sigma$  increases, (3)  $\zeta^{\text{Inst}}$  becomes greater with respect to  $p^I$ , and (4) changes in  $\zeta^{\text{Inst}}$  are not monotonic with respect to  $p^W$  for most  $p^I$ . This result would seem to imply that  $\zeta^{\text{Size}}$  and  $\zeta^{\text{Inst}}$  are correlated with each other, which would suggest that a larger size of the stationary distribution is caused by a greater stochastic periodicity made by the mechanisms inherent in the proposed day-to-day model.

Finally, we check the WDU index  $\zeta^{\text{WDU}}$  with respect to different parameters. We only adopt two parameter settings for the error term, i.e.  $(\sigma, \rho) = (0.01, 0.0)$  and  $(1.0, 0.0)$ , and observe changes in  $\zeta^{\text{WDU}}$  with respect to  $p^I$  and  $p^W$ . The results are shown in Figures 18 (where  $\sigma = 0.01$  and  $\rho = 0$ ) and 19 (where  $\sigma = 1.0$  and  $\rho = 0$ ). We can observe that  $\zeta^{\text{WDU}}$  tends to be smaller when either  $p^I$  or  $p^W$  is smaller. These results clearly indicate the changes in travellers' decisions by the WDU in the stationary distribution, despite the fact that its change can be very small when  $p^I$  and  $p^W$  are smaller.

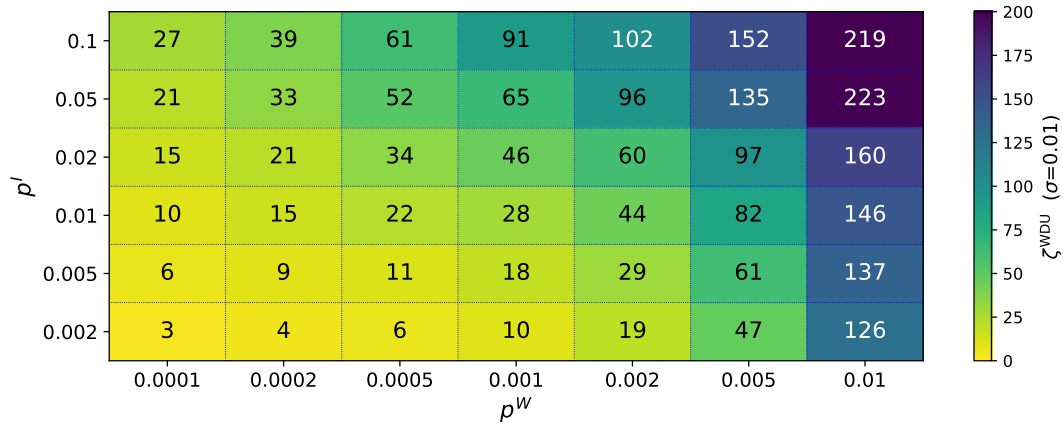


Figure 18:  $\zeta^{\text{WDU}}$  w.r.t.  $p^I$  and  $p^W$  where  $\sigma=0.01$  and  $\rho=0$

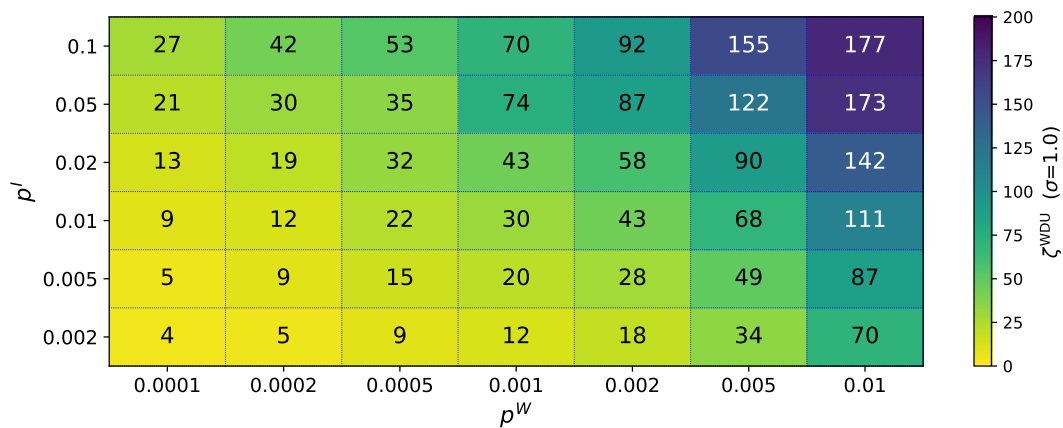


Figure 19:  $\zeta^{\text{WDU}}$  w.r.t.  $p^I$  and  $p^W$  where  $\sigma=0.01$  and  $\rho=0$

### 4.4 Adaptive resilience analysis

We explain a result related to adaptive resilience using an example case. In this example case, we assume different parameters for the departure time choice problem, in which the desired arrival time is 70 minutes after the start of the study period, the early and late penalties are  $0.1\Delta T_s$  and  $0.2\Delta T_s$ , respectively. The number of travellers is the same as in the original setting, i.e. 1800. We change the schedule cost function to emphasise the impact of the WDU when the performance of the transport system changes, i.e. smaller schedule cost coefficients would lead travellers to change their departure time when the system performance changes.

We consider an incident in which a 10-minute road closure occurs between 40 and 50 minutes after the start of the study period on a day. As defined in Section 3.4.3, this information is provided to the OTIS just after the IDM ends. We assume that travellers will be more likely to perform WDMs on this day because they would have the chance to be informed about the incident through various media, which encourages them to collect information from OTIS more frequently. To reflect this point, we replace  $p^W$  with  $p^R$  ( $p^R \geq p^W$ ) on this day only, and use 0.1, 0.01, and 0.001 for  $p^R$ . The assumed values of other parameters were as follows:  $(p^I, p^W, \sigma, \rho) = (0.01, 0.001, 0.1, 0.0)$ .

The process followed for the Monte Carlo simulation is as follows. First, pick  $\mathbf{c}(t^{\text{Max}}, d - 1)$  from a converged chain of the selected parameters. Then, simulate the IDM on day  $d$ . Then, replace  $p^{\text{W}}$  with  $p^{\text{R}}$ , and perform a simulation of day  $d$  to the end of the day, and obtain  $\mathbf{x}(t^{\text{Max}}, d)$  and the corresponding LOS. As a reference for this single-day adaptation case, we also show the stationary distribution for the same setting of the departure time choice problem. In the present paper, we only perform a qualitative comparison, although a quantitative comparison is also possible by applying the aggregations used to characterise the steady state.

The results are shown in Figures 20 to 23. We can observe that, when  $p^{\text{R}} = 0.001$ , which is the same as the  $p^{\text{W}}$ , the adaptation is very weak, in which a small number of travellers seem to defer their departure, as reflected by a peak in the incoming flow at a departure time of around 100 minutes. Once we increase  $p^{\text{R}}$  to 0.02 (20 times greater), both the incoming flow and delay profiles become more similar to those of the stationary distribution. On the other hand, when we increase  $p^{\text{R}}$  much more to 0.05, the profiles have large dispersions, implying that the effect of the WDU for the adaptation is not stable in this case.

The result implies that the resilience of the travellers' adaptation towards a new situation can be maximal when  $p^{\text{R}}$  is an appropriate number; in other words, the resilience level can be lower when  $p^{\text{R}}$  is either too small or too big. This would happen because, when  $p^{\text{R}}$  is too small, travellers' changes of choices are not sufficient, and when  $p^{\text{R}}$  is too large, large changes are made at once at each decision time step, which should lead to greater stochastic fluctuations. If an operator of the OTIS could control  $p^{\text{R}}$ , it would be suggested to seek an appropriate speed of the information provision so as to avoid sudden changes in travellers' choices.

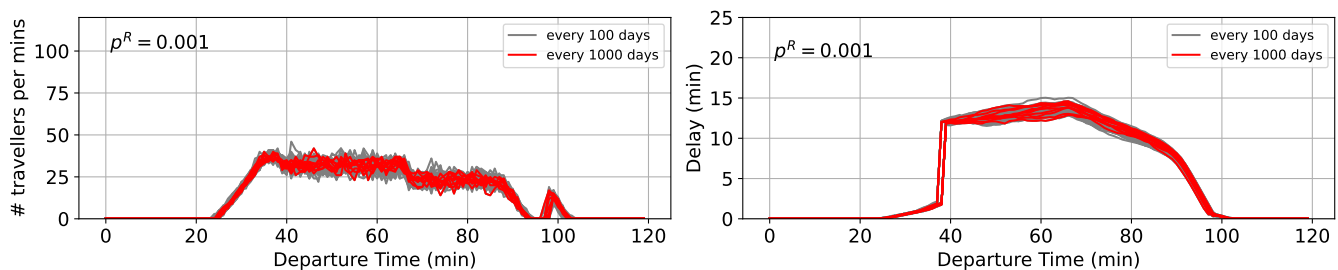


Figure 20: Incoming flow (left) and delay (right) profiles on the day of the performance change.  $p^{\text{R}} = 0.001$

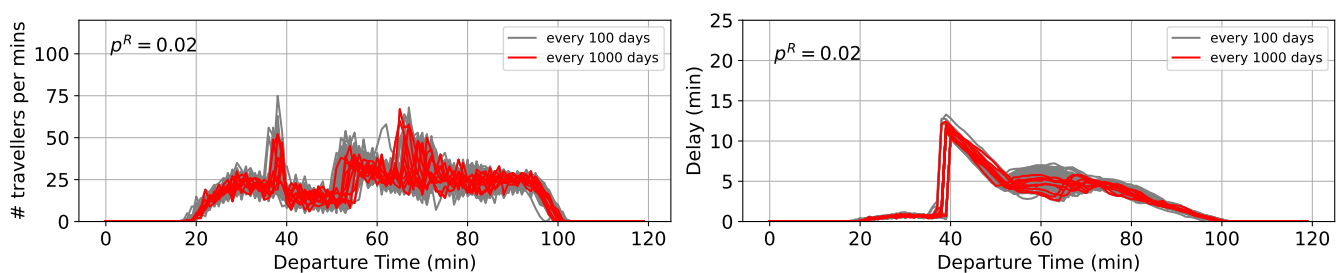


Figure 21: Incoming flow (left) and delay (right) profiles on the day of the performance change.  $p^{\text{R}} = 0.02$

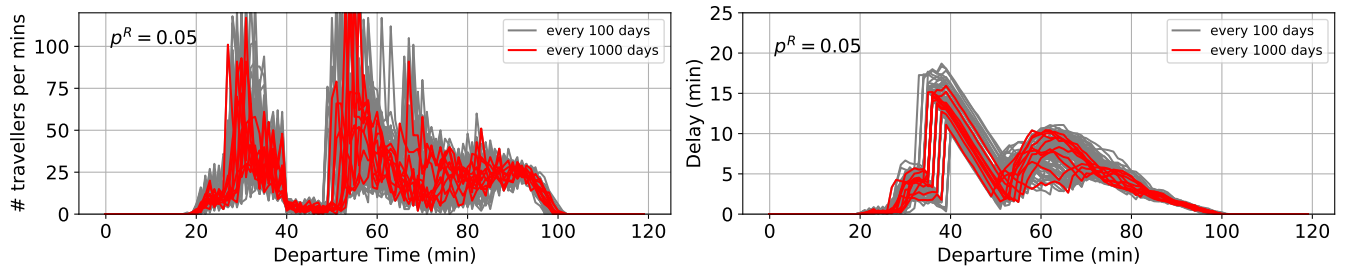


Figure 22: Incoming flow (left) and delay (right) profiles on the day of the performance change.  $p^R = 0.05$

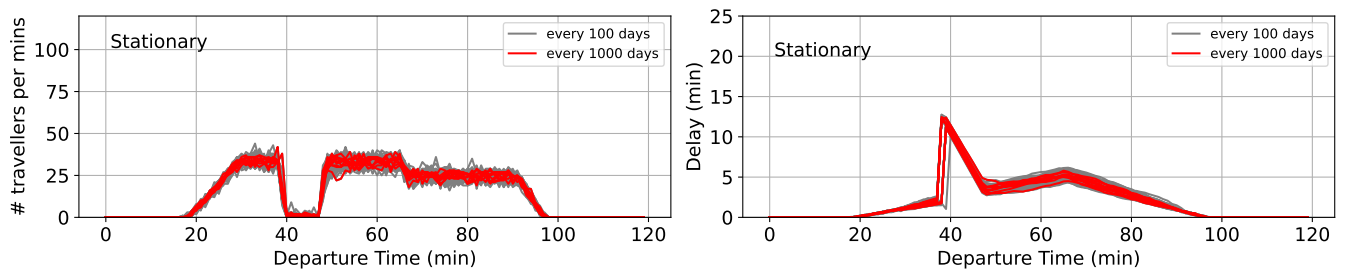


Figure 23: Incoming flow (left) and delay (right) profiles of the stationary distribution with the performance change

## 5 Network-level scalability of the proposed framework

### 5.1 Challenges and approaches for achieving network-level scalability

We discuss the challenges that arise when extending the proposed dynamical framework and the associated evaluation measures beyond the single-bottleneck problem considered in the previous section to network-wide settings. Such an extension is not straightforward, as the state representation becomes substantially more complex and the computational burden of the measures significantly increases in general road networks. To address these challenges, we propose a few approaches that facilitate network-level scalability of the framework and the measures. These approaches facilitate the adaptation of the proposed dynamical framework to network-wide settings while maintaining computational tractability and practical relevance.

#### 5.1.1 Computational challenges and countermeasures for Monte Carlo simulation

Due to the presence of the WDU, the dynamical framework requires, in the worst case, up to a factor equal to the number of time slots more computations of users' choice behaviour and LOS than the static framework. This increase in the computational load is inevitable. Therefore, for large-scale instances, it is essential to reduce the computational burden of each individual calculation as much as possible.

A simple yet effective approach is to skip the LOS calculation when changes in travellers' decisions are marginal. This strategy is particularly effective when  $p^W$  is small. We denote by  $\Delta n^{\text{ud}}$  the threshold for updating the LOS calculation, which represents the maximum number of travellers' decision updates that can be skipped before the next LOS update is performed.

For network-wide problems, special attention must be paid to the enumeration of routes. In practical computations, it is desirable to employ models that implicitly restrict the set of routes (for example, assuming that only shortest routes are used). Such approaches are practically useful. However, from a mathematical perspective, it should be noted that the assumption employed in the present study to guarantee irreducibility of the Markov chain, i.e. ‘the set of route alternatives is always fixed, and all routes within it have strictly positive choice probabilities’, is not necessarily satisfied. For network-wide problems, it is more realistic to guarantee irreducibility by using the following proposition instead.

**Proposition 1.** *Suppose the following conditions hold:*

1. *In addition to choosing a route in the route choice set implicitly generated, all travellers can choose an option not to travel.*
2. *In the initial state, the travellers’ route choice set is equal to that implicitly generated under the free-flow condition, regardless of their departure time. The set of such initial states is denoted by  $C^{\text{Initial}}$ .*
3. *The probability that all travellers perform the IDM simultaneously is positive.*

*Consider an arbitrary pair of states, denoted by  $\mathbf{c}^1$  and  $\mathbf{c}^2$ . Suppose that  $\mathbf{c}^1$  and  $\mathbf{c}^2$  are reachable within a finite number of steps from initial states  $\mathbf{c}^{\text{Init1}}$  and  $\mathbf{c}^{\text{Init2}}$ , respectively, where  $\mathbf{c}^{\text{Init1}}, \mathbf{c}^{\text{Init2}} \in C^{\text{Initial}}$ . Then,  $\mathbf{c}^2$  is reachable from  $\mathbf{c}^1$  within a finite number of steps and with positive probability.*

*Proof.* Consider the following sequence of events starting from  $\mathbf{c}^1$ :

1. *In the first chance of the IDM after  $\mathbf{c}^1$ , a transition occurs in which all travellers simultaneously update their decisions not to travel, and these decisions remain unchanged until Step 2.*
2. *In the next chance of the IDM following 1, all travellers again make decisions simultaneously, and as a result, the state becomes  $\mathbf{c}^{\text{Init2}}$ .*

The probability of the first event is positive owing to Conditions 1 and 3. Under Conditions 2 and 3, the second event also occurs with positive probability, provided that the first event leads to the free-flow condition. As  $\mathbf{c}^2$  is reachable from state  $\mathbf{c}^{\text{Init2}}$  within a finite number of transitions with positive probability, as defined, we can conclude that  $\mathbf{c}^2$  is reachable from  $\mathbf{c}^1$  within a finite number of transitions with positive probability.  $\square$

Note that the event sequence used in the proof has a positive but extremely small probability; however, this does not affect the proof of irreducibility in a theoretical sense. Conditions 1 and 3 are also not restrictive, since the associated events are only required to occur with positive probability, regardless of how small that probability is. Condition 2 may be relatively more restrictive, as it may limit the initial states that are practically relevant. However, it still permits arbitrary departure-time patterns. Moreover, restricting the route choice set to one based on free-flow conditions aligns with standard simulation practice, in which non-free-flow traffic conditions are typically not considered in the initialisation step.

### 5.1.2 Aggregation strategy for calculating the measures in network-wide instances

Aggregating the states, consisting of both the travellers' route and departure time choices, is straightforward if we adopt the *link-based aggregation*, in which link traffic volume is used to characterise the states instead of route choices or route traffic volume. Particularly, we can consider using daily link traffic volume in network-wide instances, as it can vary over days owing to travellers' route choices. This substantially reduces the dimension of the aggregated states. Note that, in the single-link setting, it is always equal to the total number of travellers and hence not useful. We may also remain in a time-dependent setting when this is of interest, while the complexity of the aggregated state also remains larger.

We can either regard a vector consisting of all links' traffic volume or that of a particular link as an aggregated state. The former approach, called *all-link-based aggregation*, is basically preferable, as it retains correlations between traffic volumes of different links, while its dimension is still large. The latter approach, called *single-link-based aggregation*, neglects this, but is suitable when observing the local situation is sufficient. It is also advantageous because depicting the result on a map is easy. We may calculate the size index of the daily link traffic volume of each link and show it on a map, which is useful to grasp which links have higher instability.

## 5.2 Numerical demonstration: a Sioux Falls case study

To demonstrate that the proposed method is scalable to practical cases, we performed a numerical case study that employed a Sioux Falls network with a multiple origin-destination (OD) pair demand pattern. The network data was prepared from the dataset available at <https://github.com/bstabler/TransportationNetworks>. The network structure and the free-flow travel times in the original data were used. The point-queue bottleneck model was employed to calculate delay at each link; its capacity was set to either 1,800 veh/hour or 900 veh/hour. To mimic morning commuter congestion, we consider a single destination (node 10; see Figure 25 for its location) in the network and assume that all travellers share an identical desired arrival time at the destination, corresponding to a common work start time. Origins are set at all nodes except node 10. The total number of travellers is 6,000, evenly distributed across all OD pairs. The deterministic route choice model was employed. Travel cost of each time slot is characterised by the travel time of the shortest route and the associated schedule cost at the destination. For calculating travellers' departure time choices, an error term was added to this travel cost in the same way as the single-bottleneck example in Section 4.

We set up three cases with different parameters. Case 1 adopted the static framework, i.e.  $p^W = 0$ , while Cases 2 and 3 adopt  $p^W = 0.002$ . We also let  $\Delta n^{\text{ud}} = 1$  and  $= 10$  for Cases 2 and 3, respectively, to evaluate the impact of skipping LOS calculations. Other parameters were commonly set as:  $p^I = 0.05$ ,  $\sigma = 0.1$ , and  $\rho = 0$ . We performed each simulation between  $d = 1$  and 1000, and picked up results for  $d \geq 501$  as its stationary state. The simulations were repeated 20 times for each parameter set.

The link-based aggregation was adopted to aggregate the state of travellers' choices. The daily traffic volume of each link on day  $d$  is denoted by  $y_l(d)$ , and its vector is denoted by  $\mathbf{y} = (y_l)_{l \in L}$ , where  $L$  is the set of links. In this case study, we examined the following two indices:

1. The size index with the all-link-based aggregation:  $\zeta_{k, \text{ALL}}^{\text{Size}}$ ,
2. The day-to-day change of Euclidean norm from the mean based on the all-link-based aggregation, denoted by  $d_{k, \text{ALL}}^{\text{Em}}(d)$

3. The size index with the single-link-based aggregation:  $\zeta_{k,l}^{\text{Size}}$ ,

where  $k = \{1, 2, 3\}$  denotes the number of the case.

We first examine the size indices to assess the size of the stationary distributions in the three cases, as summarised in Table 1. The results clearly indicate that incorporating the WDU with a positive  $p^W$  reduces the size of the stationary distribution. In addition, we analyse the day-to-day changes in the Euclidean norm,  $d_{k,\text{ALL}}^{\text{Em}}(d)$ , as illustrated in Figure 24. Large peaks are observed only in Case 1 (without WDU), suggesting that the WDU suppresses large, recurring fluctuations in the link-based aggregated state. These findings are similar to those observed in the single-bottleneck case presented in Section 4, suggesting that the effects of the WDU are also present in the network-wide case.

The results of the size indices  $\zeta_{k,l}^{\text{Size}}$  based on the single-link-based aggregation are summarised in Figures 25, 26 and Figure 27. We can observe that the average daily traffic volume of each link is almost the same across all cases. On the other hand,  $\zeta_{k,l}^{\text{Size}}$  of each link in Case 1 (without WDU) is not smaller, and typically greater, than those in Cases 2 and 3. This difference can be observed particularly around the destination node (node 10), implying that day-to-day changes of route choices in this area are more significant in Case 1 compared to the other cases.

We also observe that the results for Cases 2 and 3 differ only slightly, indicating that skipping LOS calculations reduces computational cost without a significant impact on results. In the numerical experiments for the case study, the average numbers of simulation runs per day were 50.37 for  $\Delta n^{\text{ud}} = 1$  and 28.16 for  $\Delta n^{\text{ud}} = 10$ . This corresponds to a 44% reduction in the number of simulation runs.

Table 1: Size indices calculated by all-link-based aggregation

Cases	Size index $\zeta_{k,\text{ALL}}^{\text{Size}}$
Case 1 ( $p^W = 0$ )	507.7
Case 2 ( $p^W = 0.002$ , $\Delta n^{\text{ud}} = 1$ )	236.4
Case 3 ( $p^W = 0.002$ , $\Delta n^{\text{ud}} = 10$ )	233.6

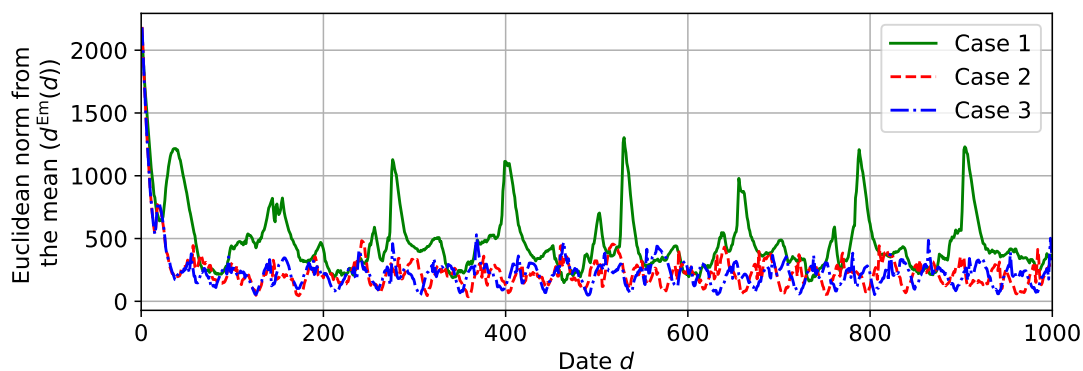


Figure 24: Euclidean distances from the means of the chains for three cases

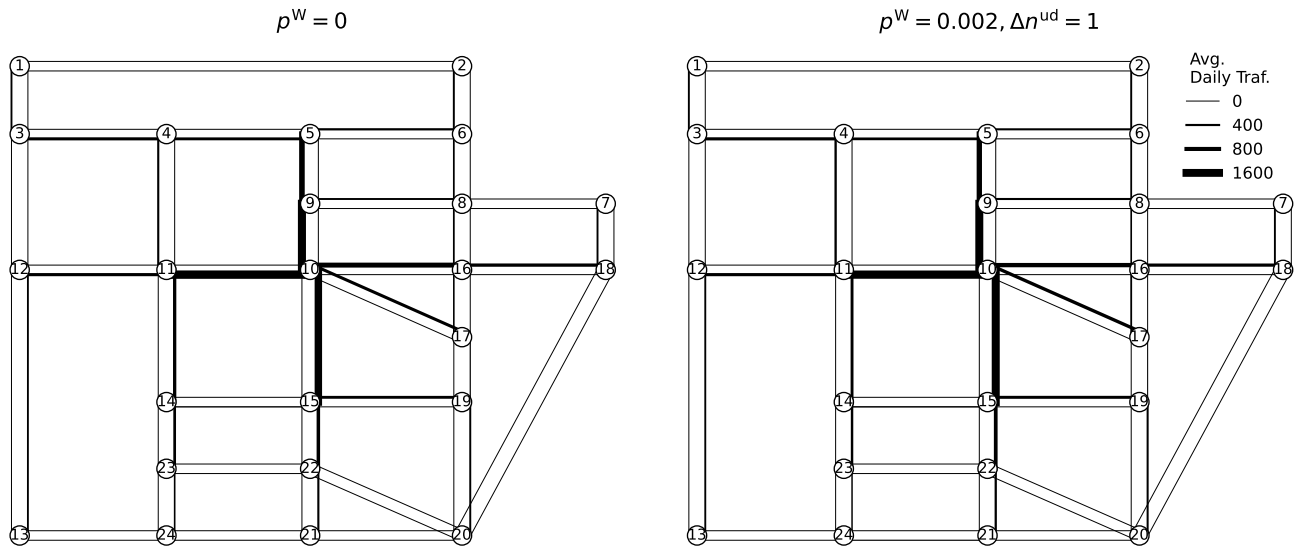


Figure 25: Average daily traffic volume of each link; left:  $p^W = 0$  (Case 1), right:  $p^W = 0.002, \Delta n^{ud} = 1$  (Case 2)

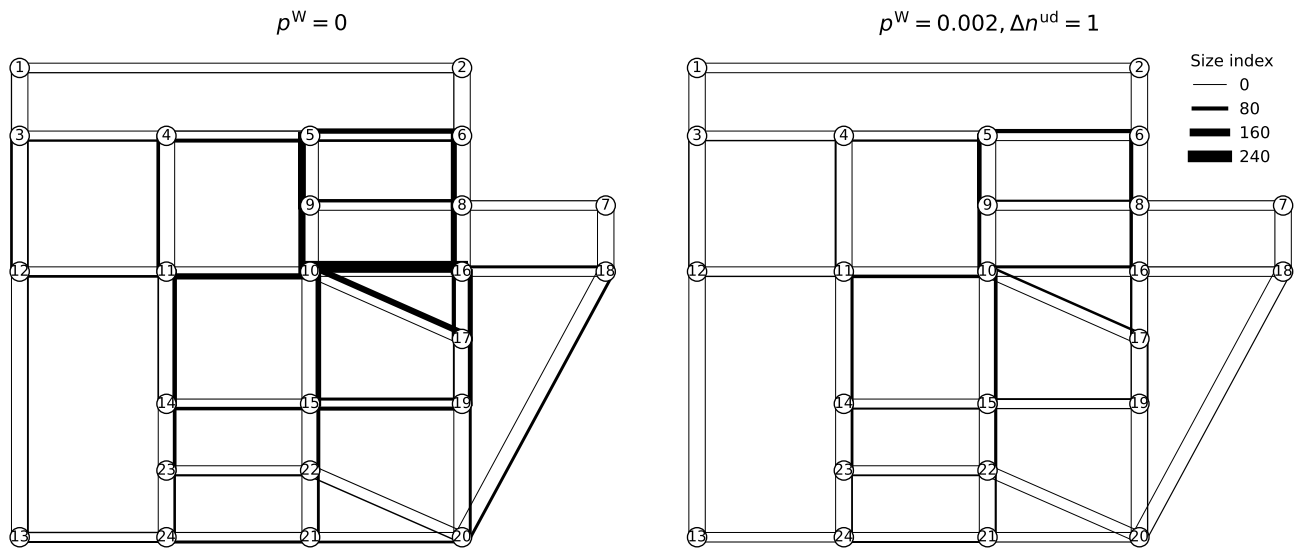


Figure 26: Size index of each link; left:  $p^W = 0$  (Case 1), right:  $p^W = 0.002, \Delta n^{ud} = 1$  (Case 2)

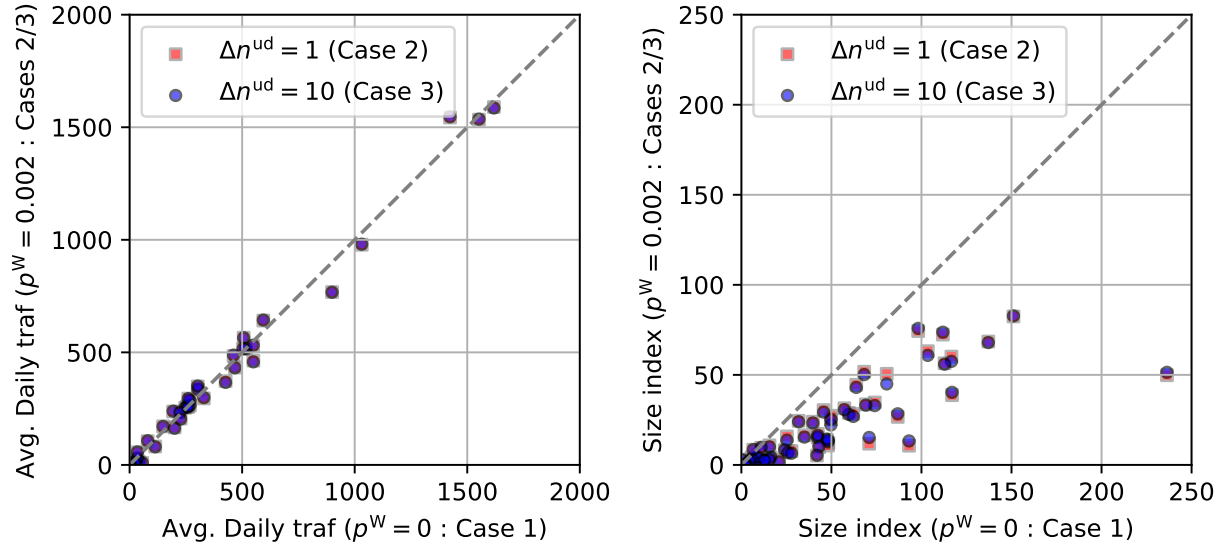


Figure 27: Scatter plot comparing average daily link traffic (left) and the size index (right) of each link among different  $k$ ; each dot corresponds to each link.

## 6 Conclusions and future directions

This study analysed the impact of including a ‘dynamical framework’ within a stochastic process model for travellers’ adjustment behaviour, whereby traveller decisions are affected not only by historical experience on previous days, but are also constrained by the within-day time at which a decision is made. The output of this study can be summarised as follows:

1. We formulated the stochastic day-to-day dynamical model incorporating the dynamical framework of decision-making. The model is simple but includes the principles of the framework, such as the decision time and shrinking property of the choice set.
2. We proposed the concept of the OTIS (Oracle Traffic Information System) as a framework to describe dynamic information provision to travellers. Although somewhat idealistic, this concept offers a clear reference point for information provision mechanisms, which can otherwise become complicated due to the wide variety of possible formalisation strategies. Furthermore, since it does not involve complex mechanisms, it has the advantage of facilitating model analysis.
3. Incorporating the concept of the OTIS, we formulated the Markov chain model describing the day-to-day dynamics with the dynamical framework. The model consists of multiple Markov chains, each of which represents the traveller’s decision-making at each decision time. We also showed that the model can be converted to a static framework model by removing a few constraints, which should be useful to make an analytical perspective regarding the impacts of the dynamical framework of decision-making.
4. We proposed multi-faceted measures describing three properties, i.e. (a) convergence speed towards the stationary distribution, (b) properties of the stationary distribution, and (c) within-day adaptation capability reflecting the resilience of the transport system.

5. As a case study of the proposed model and measures, we investigated the impacts of within-day decision-making on the day-to-day dynamics using the departure time choice problem as an example. The result clearly showed that incorporating the dynamical framework reduced both the size of the stationary distribution and stochastically periodic trends in it. We also showed that an appropriate probability of revising travellers' choices within a day improves the resilience of the transport system and travellers' behaviour in it.
6. We proposed extensions to the proposed dynamical framework and measures to the network-wide applications, and exhibited their applicability using a Sioux Falls network example. We also found that the effects of the WDU in the network-wide case are consistent with those observed in the single-bottleneck case.

These outputs are significant from a theoretical perspective. In the stochastic modelling of travellers' behaviour adjustment, which is a field with a long research history, we proposed a method that represents a doubly dynamical model in a simple and concise manner, formulated as a multiple Markov chain model. In particular, the concise description of the within-day behaviour adjustment process, enabled by the introduction of the OTIS concept, should be highly useful for future theoretical studies. The fact that the doubly dynamical model can be mathematically reduced to existing day-to-day dynamical models by relaxing certain conditions helps clarify the significance of incorporating within-day dynamics. Furthermore, this study offers a numerical methodology for analysing the stability of the departure time problem, which has long been known for its instability. Recent attempts to maintain the stability of departure time choice problems include works by Iryo et al. (2020), Jin (2020), Jin (2021), and Satsukawa et al. (2024). Our study adds implications regarding stabilisation from a different perspective.

Although this research is primarily aimed at obtaining theoretical insights, the results also provide practical implications that will be important for the future operation of advanced transport systems assisted with information communication technologies. With technological advancements, all transport agents, both vehicles and individual persons, are becoming increasingly interconnected, and this involves continuous and intensive communications between them. The development of automated transport systems, currently represented by autonomous vehicles, is expected to expand from vehicle control to more strategic decisions such as route and departure time choices. The unstable behaviour of such large-scale, automated, and connected transport systems has negative impacts on society. The methodology proposed in this study is expected to serve as a theoretical foundation for analysing the stability of such systems and for developing measures to ensure their stability.

Lastly, we note several future challenges. The OTIS framework proposed in this study allows us to obtain travellers' decisions immediately upon their decision-making, but it does not allow for the prediction of decisions to be made in the future. In the resilience analysis presented in Section 4.4, it was shown that when many travellers attempt to update their decisions simultaneously, the stability of the system deteriorates. This phenomenon may be attributed to the unpredictability of future decisions by OTIS. If a more 'oracle-like' OTIS model is developed, it would enable the evaluation of the impact of predicting travellers' future behaviour on system stability. The proposed model incorporates parameters and sub-models that describe travellers' information-collection processes, although in the numerical studies, we used settings that are reasonable but hypothetical. Conducting behavioural surveys would provide a straightforward way to use actual data to determine how the IDM/WDU is embedded in travellers' behaviour and whether it has a substantial effect in practice. On the other hand, as discussed earlier, technological advancements may enable the real-time collection of such data in transport systems where all agents are interconnected in the future. In a more extreme scenario, the IDM/WDU could be automated and controlled by such sys-

tems, without human intervention, to improve overall transport system performance, including reliability and resilience. In this case, the proposed method could be used to design detailed IDM/WDU algorithms, in which the IDM/WDU would no longer be a thing to be estimated but rather optimised by the system.

## Acknowledgement

This study was financially supported by JSPS Grant-in-Aid #25H00751.

## CRedit authorship contribution statement

**Takamasa Iryo:** Conceptualisation, Methodology, Software, Visualisation, Formal analysis, Writing - Original Draft, Writing - Review and Editing, Funding Acquisition. **David Watling:** Conceptualisation, Methodology, Writing - Review and Editing. **Martin Hazelton:** Conceptualisation, Methodology, Writing - Review and Editing.

## References

- Cantarella, G., Fiori, C., and Velona, P. (2025). Moving average vs. exponential smoothing cost-updating filters for day-to-day dynamic assignment: fixed-point stability and bifurcation theoretical analysis. *Transportation Research Part B: Methodological*, 199:103253.
- Cantarella, G. E. and Cascetta, E. (1995). Dynamic processes and equilibrium in transportation networks: Towards a unifying theory. *Transportation Science*, 29(4):305–329.
- Cantarella, G. E. and Watling, D. P. (2015). Model representation and decision-making in an ever-changing world: The role of stochastic process models of transportation systems. *Networks and Spatial Economics*, 15:843–882.
- Cascetta, E. (1989). A stochastic process approach to the analysis of temporal dynamics in transportation networks. *Transportation Research Part B*, 23(1):1–17.
- Chang, G.-L. and Mahmassani, H. S. (1988). Travel time prediction and departure time adjustment behavior dynamics in a congested traffic system. *Transportation Research Part B: Methodological*, 22(3):217–232.
- Chen, L., Wang, Y., and Ma, D. (2021). A dynamic day-to-day departure time and route choice model for bounded-rational individuals. *Mathematical Problems in Engineering*, 2021(1):6686843.
- Friesz, T., Kim, T., Kwon, C., and Rigdon, M. (2011). Approximate network loading and dual-time-scale dynamic user equilibrium. *Transportation Research Part B: Methodological*, 45(1):176–207.
- Friesz, T. L., Bernstein, D., Mehta, N. J., and Tobin, R. L. (1994). Day-to-day dynamic network disequilibria and idealized traveler information systems. *Operations Research*, 42(6):1120–1136.
- Friesz, T. L., Bernstein, D., and Stough, R. (1996). Dynamic systems, variational inequalities and control theoretic models for predicting time-varying urban network flows. *Transportation Science*, 30(1):14–31.

- Guo, R.-Y., Yang, H., and Huang, H.-J. (2018). Are we really solving the dynamic traffic equilibrium problem with a departure time choice? *Transportation Science*, 52(3):603–620.
- Hazelton, M. L. (2002). Day-to-day variation in Markovian traffic assignment models. *Transportation Research Part B*, 36(7):637–648.
- Hazelton, M. L. and Watling, D. P. (2004). Computation of equilibrium distributions of markov traffic-assignment models. *Transportation Science*, 38(3):331–342.
- He, X., Guo, X., and Liu, H. X. (2010). A link-based day-to-day traffic assignment model. *Transportation Research Part B*, 44(4):597–608.
- Horowitz, J. L. (1984). The stability of stochastic equilibrium in a two-link transportation network. *Transportation Research Part B*, 18(1):13–28.
- Iryo, T. (2008). An analysis of instability in a departure time choice problem. *Journal of Advanced Transportation*, 42(3):333–356.
- Iryo, T. (2019). Instability of departure time choice problem: A case with replicator dynamics. *Transportation Research Part B*, 126:353–364.
- Iryo, T., Smith, M. J., and Watling, D. (2020). Stabilisation strategy for unstable transport systems under general evolutionary dynamics. *Transportation Research Part B: Methodological*, 132:136–151.
- Iryo, T., Watling, D., and Hazelton, M. (2024). Estimating Markov chain mixing times: Convergence rate towards equilibrium of a stochastic process traffic assignment model. *Transportation Science*, 58(6):1168–1192.
- Jin, W.-L. (2007). A dynamical system model of the traffic assignment problem. *Transportation Research Part B: Methodological*, 41(1):32–48.
- Jin, W.-L. (2020). Stable day-to-day dynamics for departure time choice. *Transportation Science*, 54(1):42–61.
- Jin, W.-L. (2021). Stable local dynamics for day-to-day departure time choice. *Transportation Research Part B*, 149:463–479.
- Lamotte, R. and Geroliminis, N. (2021). Monotonicity in the trip scheduling problem. *Transportation Research Part B: Methodological*, 146:14–25.
- Levin, D. A. and Peres, Y. (2017). *Markov chains and mixing times*, volume 107. American Mathematical Society, Providence, RI, USA.
- Li, J., Wang, Q., Feng, L., Xie, J., and Nie, Y. M. (2024). A day-to-day dynamical approach to the most likely user equilibrium problem. *Transportation Science*, 58(6):1193–1213.
- Li, M., Lu, J., Sun, J., and Tu, Q. (2019). Day-to-day evolution of traffic flow with dynamic rerouting in degradable transport network. *Journal of Advanced Transportation*, 2019(1):1524178.
- Mahmassani, H. S. and Chang, G.-L. (1986). Experiments with departure time choice dynamics of urban commuters. *Transportation Research Part B*, 20(4):297–320.

- Parry, K., Watling, D. P., and Hazelton, M. L. (2016). A new class of doubly stochastic day-to-day dynamic traffic assignment models. *EURO Journal on Transportation and Logistics*, 5(1):5–23.
- Satsukawa, K., Wada, K., and Iryo, T. (2019). Stochastic stability of dynamic user equilibrium in unidirectional networks: Weakly acyclic game approach. *Transportation Research Part B*, 125:229–247.
- Satsukawa, K., Wada, K., and Iryo, T. (2024). Stability analysis of a departure time choice problem with atomic vehicle models. *Transportation Research Part B: Methodological*, 189:103039. *Transportation Research Part B: Methodological - ISTTT25*.
- Smith, M. J. and Watling, D. P. (2016). A route-swapping dynamical system and Lyapunov function for stochastic user equilibrium. *Transportation Research Part B: Methodological*, 85:132–141.
- Watling, D. (1996). Asymmetric problems and stochastic process models of traffic assignment. *Transportation Research Part B: Methodological*, 30(5):339–357.
- Watling, D. P. and Cantarella, G. E. (2013). Modelling sources of variation in transportation systems: theoretical foundations of day-to-day dynamic models. *Transportmetrica B: Transport Dynamics*, 1(1):3–32.
- Watling, D. P. and Hazelton, M. L. (2018). Asymptotic approximations of transient behaviour for day-to-day traffic models. *Transportation Research Part B*, 118:90–105.
- Yang, F. and Zhang, D. (2009). Day-to-day stationary link flow pattern. *Transportation Research Part B: Methodological*, 43(1):119–126.